

Detail Design Report

AERODYNAMICS

April 24, 2024



Department of Mechanical, Industrial and Aerospace Engineering,
Concordia University
Montreal, QC, Canada

Contents

1 Requirements	1
2 Design	1
2.1 Wing re-sizing	2
2.2 Wing, Winglet and Fuselage Design	2
2.3 Performance and Load Distribution Analysis	2
2.3.1 Control Surface Definition	2
2.3.2 Static and Dynamic Stability Analysis	3
2.4 Aircraft Final Geometries	3
3 Test Plan	4
4 Conclusion	5
Appendices	7
A Aerodynamic Team-Specific Requirements	7
B OML	9
B.1 Wing Design	9
B.2 Winglet Design	12
B.3 Fuselage Design	13
B.4 Empennage Design	13
B.5 Control Surface Design	17
B.5.1 Ailerons	17
B.5.2 Ruddervators	20
B.6 Fairings, Blisters and Openings	21
C Performance and Load Analysis	22
C.1 Stability	22
C.1.1 Static Stability	22
C.1.2 Dynamic Stability	24
D Computational Fluid Dynamics	29
D.1 Geometry for CFD	29
D.2 Domain Geometry	29
D.3 Mesh Independence Study	30
D.4 Meshing Strategies	30
D.5 CFD Results	32
D.5.1 Aircraft Performance	32
D.5.2 Aircraft Roll	33
D.5.3 Aircraft Pitch and Yaw	34
E Test Plan	38
E.1 Introduction	39
E.1.1 Background	39
E.1.2 Test Item Description	39
E.2 Test Resource Requirements	39
E.2.1 Test Facilities, Ranges and Resources	40

E.2.2	Test System/Aircraft	40
E.2.3	Instrumentation and Parameter requirements	40
E.2.4	Support Vehicles/Aircraft	40
E.2.5	Safety Considerations	40
E.2.6	Security requirements	40
E.2.7	Key stakeholders contact information	40
E.2.8	Test Environment Requirements	41
E.2.9	Environmental Impact Assessment	41
E.3	TEST AND EVALUATION	41
E.3.1	General Test Objectives (GTOs) and Specific Test Objectives (STOs)	41
E.3.2	Potential Impacts of Completion Criteria	43
E.4	GTO 1 – Validation testing of designed drone’s aerodynamic performance	43
E.4.1	STO 1.1– Validation testing of lift coefficient of the airfoil	43
E.4.2	STO 1.2 – Validation testing of the lift from the wing	44
E.5	GTO 2 – Validation testing of designed drone’s maneuverability and stability	44
E.5.1	STO 2.1– Validation testing of tail static stability	44
E.5.2	STO 2.2– Validation testing of tail stability during maneuvers	45
E.5.3	STO 2.3– Validation testing of tail rolling moment during maneuvers	46
E.5.4	STO 2.4– Validation testing of aileron roll rate for maneuverability.	47
E.5.5	STO 2.5– Validation testing of ruddervator pitch rate	48
E.6	TEST CONDUCT	49
E.6.1	Readiness reviews	49
E.6.2	Pretest Briefing(s)	50
E.6.3	Test execution	51
E.6.4	Post-test Briefing	51
E.6.5	Post-test Data Procedures	51
E.7	Test Reporting	51
E.7.1	4.1 Data deficiency reporting	51
E.7.2	Quick look reports	52
E.7.3	Preliminary Report of Results	52
E.7.4	Capability report	52
E.7.5	Technical Information Memorandum/Handbook	52
E.7.6	Technical Report (TR)	52
E.7.7	Data packages (DP)	52
E.7.8	Test completion letter (TCL)	52
E.8	List of Acronyms and Abbreviations for Test Plan	53
E.9	Nomenclature for Test Plan	53
E.10	Disturbance maneuvers	53
F	Aircraft Drawings	56

List of Figures

1	Detailed Design Process - XDSM	1
2	Aircraft Models	4
B.1	Design Structure Matrix	10
B.2	Wing Airfoil - FX 63-137	10
B.3	FX 63-137 Aerodynamic vs. AOA	11
B.4	Updated constraint diagram	12
B.5	Winglet Design Process	12
B.6	Fuselage Design Process	13
B.7	Tail sizing methodology	14
B.8	Inverted V-Tail Airfoil - NACA 0012	17
B.9	Deflected Left Aileron seen a) from behind; b) from above; c) isometrically	18
B.10	Empennage with Ruddervator Model	21
C.1	C _{mo} vs AOA plot	23
C.2	Complex plane for lateral modes	27
C.3	Complex plane for longitudinal modes	28
D.1	Simplified Geometry for CFD	29
D.2	Flow Geometry Domain - (not to scale).	29
D.3	Mesh Independence Study Plot	30
D.4	Mesh Results Obtained after Mesh Independence Study	31
D.5	Lift Coefficient vs. Angle of Attack - Wing Comparison.	32
D.6	Lift Coefficient vs. Angle of Attack - UAV.	33
D.7	Drag Polar - UAV.	33
D.8	Total Pressure Contours for Yaw right	35
D.9	Static Pressure Contours for Pitch Up	36
D.10	Local Velocity Contours for Pitch Up	37
E.1	Schematic of Phugoid and Short-Period Oscillation [10]	53
E.2	Dutch Roll Schematic [7]	54
E.3	Sideslip schematic[5]	55

List of Tables

1	Dynamic Stability Characteristics	3
2	Aircraft Final Geometries	4
B.1	Part List for the OML DMU	9
B.2	V-tail dimensions	17
B.3	Comparison of Results from Hand-Calculations and CFD	18
B.4	Results of CFD simulations made with the old configuration	19
C.1	Static stability results	23
C.2	Aircraft's moment of inertia	23
C.3	Phugoid Mode Requirements [12].	24
C.4	Roll Mode Time Constant Specification (Maximum Value)[12]	25
C.5	Time to double amplitude in spiral mode [12]	25
C.6	Dutch-Roll Mode Handling Qualities [12]	26
C.7	Dynamic Stability Characteristics	26
D.1	Mesh Independence Study Results	30
D.2	Final Mesh Settings and Setup	31
D.3	Results of the Simulations with the Ailerons at a 20-degree Inclination	34
D.4	CFD Results for Pitch and Yaw	34

E.1	List of delegates supervising and executing the tests	41
E.2	General Test Objectives (GTOs) and Specific Test objectives (STOs)	42
E.3	Rolling moment expected results for different flight conditions.	47

Abbreviations

<i>UAV</i>	-	Unmanned Aerial Vehicle
<i>XDSM</i>	-	eXtended Design Structure Matrix
<i>MDO</i>	-	Multi-Disciplinary Design Optimization
<i>CFD</i>	-	Computational Fluid Dynamics
<i>BEMT</i>	-	Blade Element Momentum Theory
<i>MRF</i>	-	Multi-Reference Frames
<i>MTOW</i>	-	Maximum Takeoff Weight
<i>RFP</i>	-	Request For Proposal
<i>AOA</i>	-	Angle of Attack
<i>C&C</i>	-	Command and Control
<i>OML</i>	-	Outer Mold Line
<i>DMU</i>	-	Digital Mock-Up
<i>MAC</i>	-	Mean Aerodynamic Chord

Nomenclature

α	-	Angle of Attack
δ	-	Control Surface Deflection Angle
L	-	Lift Force
D	-	Drag Force
C_L	-	Lift Coefficient
C_D	-	Drag Coefficient
C_L/C_D	-	Lift-to-drag ratio
L/D	-	Lift-to-drag ratio
T/W	-	Thrust-to-weight ratio
W/S	-	Wing Loading
Re	-	Reynold's Number
b	-	Wing Span
C_r	-	Root Chord
C_t	-	Tip Chord
S	-	Reference Area

1 Requirements

To ensure the aerodynamic team's designs align seamlessly with the goals set by the customers and the drone performs as intended, requirements must be established at every level—from overall aircraft specs down to the specifics of individual components. Since designs go through iterations, it's easy to lose track of these requirements. That's where a traceability framework comes in, ensuring each design aspect has a rationale linked directly or indirectly to a specific requirement.

Take the MTOW as an example. It's not just a basic design spec; it ripples across the whole design, affecting the airfoil, wing size, and even how secondary control surfaces are configured. This showcases how requirements branch out.

For verification and validation, the designs must be able to be tested against a quantifiable test requirement thus categorizing the test as a pass or fail. This way, a design either aligns with the traced requirement or, if not, prompts a redesign to meet both individual and overarching requirements.

It's also worth noting that some requirements and objectives come from constraints set by other disciplines. Their outputs often feed into aerodynamic design directly. For instance, the pusher motor needing enough thrust for flight at 4,000 meters is an objective to cut down on drag. This objective, stemming from the RFP, aims to lighten the load for the propulsion team, offering more design options. It's a ripple effect where the RFP indirectly influences the objective.

To ensure that the drone operates as expected, it is designed to handle the most extreme conditions laid out by the RFP.

Safety factors are crucial but stacked cautiously with the aim of attaining the right balance between safety measures and streamlined design principles, avoiding unnecessary safety factor overload.

See appendix A for further details.

The detail design phase obtained inputs from the preliminary design and this led to the final design of different aircraft components related to the aerodynamics group, namely the wing, winglets, fuselage and the tail.

2 Design

The following XDSM diagram shows the methodology followed by aerodynamics group for detailed design. The main focus of the detail design was to make the aircraft stable while keeping the changes in this phases to a minimum.

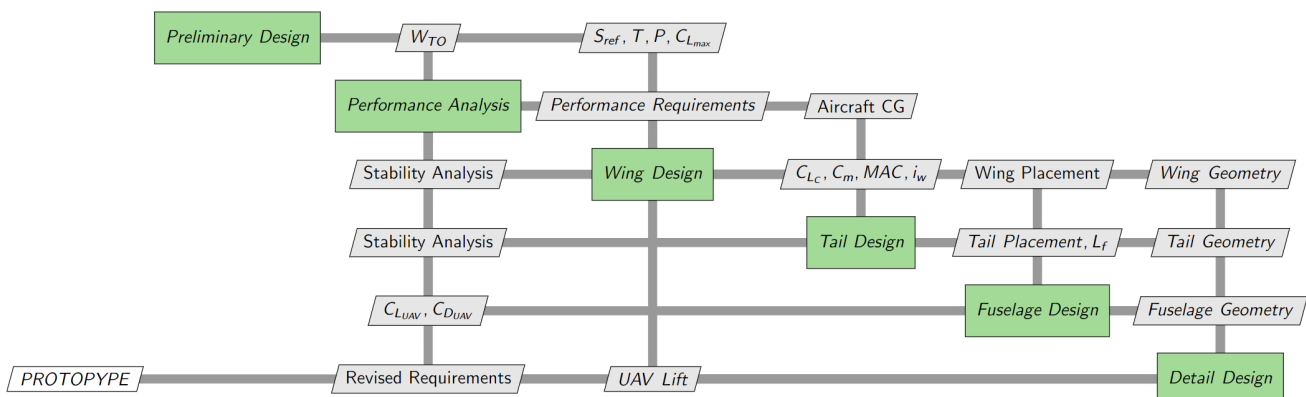


Figure 1: Detailed Design Process - XDSM

2.1 Wing re-sizing

It was determined that due to weight increase, the 1.7 meter wing span cannot produce enough lift. Thus through memo 6. The design was amended and the wing span was increased to 2 meters while keeping the other dimensions the same. The tail was not resized. In the following section, stability static, and dynamic were investigated to determine if the decision of not resizing the tail is appropriate.

2.2 Wing, Winglet and Fuselage Design

The wing was resized based on the information provided in subsection 2.1. This provided a 2m wingspan rectangular wing. Detail design of wing has been discussed in subsection B.1 along with rationale behind airfoil selection. Additionally, the winglets were added to the design to enhance the vehicle's aerodynamic performance. The addition of the winglets reduced the aircraft's lift induced drag while leading to a higher values of lift-to-drag ration. The methodology of the winglet design has been discussed in detail in subsection B.2. The performance enhancement results due to winglets were obtained from detailed CFD of the wing and have been discussed on subsection D.5.

2.3 Performance and Load Distribution Analysis

2.3.1 Control Surface Definition

To define the initial size of the ailerons, a set of assumptions and benchmarking data was used. Then, through a series of hand-calculations, the roll moment and the time necessary to make a 30-degree bank angle change was determined. That procedure was expanded upon in detail in the preliminary design report. It follows the procedure seen in Sadraey (2012), page 669 [12]. The final sizing and position of the aileron can be seen in figure B.9. For the detailed design, CFD was used to produce the roll moment. The procedure used and the full analysis of the results can be found in section B.5.1. In summary, the data from cfd confirmed that the aileron would be able to provide sufficient roll control. The projected time for the aircraft to perform a 30-degree bank angle change is between 0.3430 and 0.4979 depending on the altitude and speed. This is below the requirement of 1.3 seconds, even when a safety factor of 2 is used.

Moreover, the actuator can produce a high enough torque to move the aileron in normal operating conditions. The maximum torque the actuator can provide is 13.06 kg-cm, which is above the 3.1985 kg-cm obtained from CFD. Even with a safety factor of 2, the actuator is able to move the aileron under that load. However, at dive conditions, the hinge moment that occurs is 9.01 kg-cm. With a safety factor of 2, this becomes 18.02 kg-cm, which yields a maximum safety factor of only 1.44. This safety factor should still be sufficient because the ailerons are not necessarily used to their maximum deflection angle in dive conditions. However, it is still something that will be monitored in collaboration with C&C. The calculation of the hinge moment from the forces acting on the aileron can be seen in section B.5.1.

The maximum possible aerodynamic forces acting on the aileron are $D = 11.60 \text{ N}$ and $L = 23.54 \text{ N}$, which make for a total maximum force of 26.24 N acting on the aileron. According to the Airframes 1 team, this number is realistic for the aileron. Although they would need to do more simulations and testing to be sure, the ailerons should be able to resist such a load.

The ruddervator sizing method,better explained in B.5.2, was based on insights from comparable drones, resulting in specific dimensions. ANSYS simulations were used to analyze the design's performance in critical scenarios. Computational Fluid Dynamics (CFD) and XFLR5 methodologies were employed for hinge moment calculations, favouring XFLR5 for its precision. Validation of ruddervator sizing and visualization of moments will be conducted using XPLANE simulation software, ensuring compliance with the pitch rate requirement. This comprehensive approach enhances the design's accuracy and performance. Figure B.10 shows the ruddervator size in proportion to the overall empennage.

2.3.2 Static and Dynamic Stability Analysis

Static stability results and dynamic stability results are summarized in this section. For the complete comprehensive analysis refer to subsection C.1.

Static stability summary

$$X_{CP} = 0.08 \text{ m from the leading edge} = 33\% \text{ of the MAC}$$

$$X_{NP} = 0.173 \text{ m from the leading edge} = 71\% \text{ of the MAC}$$

$$X_{CG} = 0.144 \text{ m from the leading edge} = 59\% \text{ of the MAC}$$

$$X_{CG_FWD} = 0.09 \text{ m from the leading edge} = 37\% \text{ of the MAC}$$

$$SM = \frac{X_{NP} - X_{CG}}{MAC_w} = \frac{0.173 - 0.144}{0.2242} = 0.12$$

Dynamic stability summary

Table 1: Dynamic Stability Characteristics

Maneuver	Real	Imaginary	ζ	ω_d	ω_n	T_r	t_2
Short period Phugoid	-2.170	± 3.80	0.496	0.605	0.697	-	-
Long period Phugoid	0.009	± 0.77	0.013	0.124	0.124	-	-
Roll	-6.800	0	-	-	-	0.147	0.102
Dutch roll	-1.020	± 1.72	0.502	0.278	0.322	-	-
Spiral	0.577	0.000	-	-	-	-	12.010

The unmmanned UAV lies under category (II) homebuilt. With this consideration, we can compare the results in table C.7 to the tables above described

1. Short period Phugoid mode: $\zeta_{ph} = 0.496$. Therefore, the level of acceptance is 1. Meaning the airplane is stable in this maneuver, and the pilot would be very comfortable with this perturbation.
2. Long period Phugoid mode: $\zeta_{ph} = 0.013$. Therefore, the level of acceptance is 2. Meaning the airplane is stable in this maneuver, but the pilot would be hardly comfortable with this perturbation.
3. Roll subsidence mode: $T_r = 0.147$. This value is less than 1 and 1.4 at every flight phase. So, the level of acceptance is 1. Meaning the airplane is stable in this maneuver and the pilot would be very comfortable with this perturbation.
4. Dutch roll oscillation mode: $\zeta_d = 0.502$. This value is more than 0.19 and 0.08 at every flight phase. Therefore, the level of acceptance is 1. Similarly, $\zeta_d \times \omega_{nd} = 0.16$. This value is bigger than 0.15 but less than 0.35. Therefore, the overall level of acceptance is 2. Meaning the airplane is stable in this maneuver, but the pilot would be hardly comfortable with this perturbation.
5. Spiral mode: $t_2 = 12.01$ s which lies on level 2 of acceptability. Meaning the time to double amplitude is acceptable. Thus, no correction to the V-tail is needed because the Pixhawk autopilot should be able to correct this perturbation.

2.4 Aircraft Final Geometries

The final geometries of the aircraft can be found in Table 2. The detailed analysis can be found in the appendices attached with this report. A 22 % scaled model was produced as a mock-up to get an idea of the aircraft geometries. The scaled model can be seen in Figure 2a. The digital mock-up can be seen in Figure 2b. Both models

have propellers placed properly in order to show the clearances. Additionally, detailed drawings of the UAV are presented in Appendix F.

Table 2: Aircraft Final Geometries

Parameter	Value	Units	Parameter	Value	Units
FUSELAGE					
Length	0.640	[m]			
Maximum Diameter	0.170	[m]			
WING			EMPENNAGE		
Span	2.000	[m]	Tail Arm Length	0.886	[m]
MAC	0.242	[m]	Span	0.83	[m]
Root chord	0.242	[m]	MAC	0.155	[m]
Tip chord	0.242	[m]	Surface area	0.113	[m ²]
Surface area	0.484	[m ²]	Aspect ratio	6.7	[deg]
Aspect ratio	8.264	[/]	V-Tail angle	27.3	[deg]
Tail setting angle	0.0	[deg]	Z position correction	0.145	[m]
Airfoil	FX 63-137	[/]	Airfoil	NACA 0012	[/]



Figure 2: Aircraft Models

3 Test Plan

The test plan (provided in the appendices) follows the format provided by 412TW-PA-21099 U.S AIRFOIRCE Technical Information Handbook titled “Test Plan Author’s Guide” [8]. Any formulation of section titles similar to the template provided by the aforementioned military standard is intentional for a clear depiction of the presented information. Distribution has been permitted by any authoring parties. Compliance with regional (Canadian) standards needs to be checked.

4 Conclusion

During the detailed design, a list of disciplinary and interdisciplinary requirements (for all aircraft design levels) has been established. This list of requirements can be traced back to the requirements from the integration team and includes the validation testing methods of each requirement. Furthermore, a test plan has been drafted with more details on the tests and their methodologies in the appendices. In terms of sizing, the wingspan was increased from 1.7 m to 2 m to generate sufficient lift. The tail and aileron sizing has not been changed, but ruddervator sizing was finally achieved. The control surfaces specifications describing their contribution to the overall maneuverability (e.g. rolling moment, actuation loads, pitch rates, etc.) were determined analytically (using benchmarking and calculations) as well as computationally (using Ansys CFD and XFLR5). In addition to updating the static stability margin based on new sizing, the dynamic stability analysis was also carried out. The dynamic stability analysis determined that the drone was stable during 2 critical lateral perturbances and 3 longitudinal perturbances (e.g. short-to-long period phugoid mode, Dutch roll, etc.). Lastly, the digital mock up dimensions were finalized, and a 3D model reflecting the final dimensions of the entire drone body was printed at a 22% scale.

References

- [1] Building aerodynamica/ wind tunnel lab. <https://www.concordia.ca/ginacody/building-civil-environmental-eng/research/building-aerodynamics-wind-tunnel-lab/facilities-equipment.html>. Accessed: 2023-11-27.
- [2] How to measure control surface deflection angle on small uavs. <https://www.aerospacetestinginternational.com/features/how-to-measure-control-surface-deflection-angle-on-small-uavs.html>. Accessed: 2023-11-27.
- [3] "load cells"-transducer techniques. <https://www.transducertechniques.com/load-cell.aspx>. Accessed: 2023-11-27.
- [4] "load cells"-transducer techniques. <https://www.aerospacetestinginternational.com/features/how-to-measure-control-surface-deflection-angle-on-small-uavs.html>. Accessed: 2023-11-27.
- [5] "slips – forward and side". <https://flighttrainingcenters.com/training-aids/private-pilot/pre-solo/slips-forward-and-side/>. Accessed: 2023-12-02.
- [6] Amazon. Jx servo 8kg/9kg/13kg/15kg/20kg high torque metal gear standard servo for helicopter drone tank car robot accessories (pdi-5513mg/13kg), 2023. Accessed on April 24, 2024.
- [7] Michael V. Cook. *Flight Dynamics Principles A Linear Systems Approach to Aircraft Stability and Control*, 3rd ed. Butterworth-Heinemann, 2013. Chapter 7.
- [8] C. J. Liebmann S. S. Mailen J. D. Martin G. Van Peteghem, D. W. Osburn and K. L. Peck. Test plan author's guide. Technical report, Office of the Technical Director, United States Air Force (412th Test Wing), 2021.
- [9] S. Khadka, J. I. Abeygoonewardene, and N. P. Liyanage. Conceptual design of boom mounted inverted v-tail in the searcher mk ii uav. *Name of the Journal*, 2020.
- [10] A. K. Kundu. *Aircraft Design*. Cambridge Aerospace series. Cambridge Press, Cambridge, 2010. 12.6 Inherent Aircraft Motions as Characteristics of Design, p.404-405.
- [11] Daniel P. Raymer. *Simplified Aircraft Design for Homebuilders*. Design Dimension Press, 2002.
- [12] Mohammad H. Sadraey. *Aircraft Design: A Systems Engineering Approach*. Aerospace series. Wiley, Hoboken, New Jersey, 2012. 1 online resource.
- [13] Airfoil Tools. Airfoil tools, Year. Accessed on April 24, 2024.

APPENDICES

A Aerodynamic Team-Specific Requirements

The Aerodynamics team-specific requirements were derived from various sources including the RFP, external scholarly references such the Sadraey textbook and integration-specific design choices to fit the wants and needs of the customer(s).

Space left blank on purpose. The following page shows the requirements summarized for aerodynamics group.

Component	ID	Requirement Discipline	Requirement Description	Trace	Verification	Validation	Location	Rationale
Wing	W-Af-1	Airfoil	Airfoil shall provide a maximum lift coefficient of at least 1.5	Sadraey	Thin airfoil theory estimations	Wind tunnel testing	Concordia Hall Building	Categorical data (Sadraey Table 4.11)
	W-Af-2		The airfoil design shall be capable of achieving a climb rate of at least 2 m/s to an altitude of 500 m AGL	S-WING-005			Concordia Hall Building	
	W-S-1	Size	The wing shall be large enough to provide 92 N of lift at altitudes up to 4'000m ASL.	A-GEN-001, RFP-SP01, A-GEN-002, RFP-SP03	CFD	Wind tunnel testing	Concordia Hall Building	Mission profile - sufficient lift at max altitude -> ensures sufficient lift throughout
	W-S-2		Weight of the wing shall be carefully considered to ensure enough weight allocation for other components while meeting weight allowance	A-GEN-001 , RFP-SP01	CAD	Assembly	Aero Lab EV Building	As long as the MTOW and structural integrity is met
	W-S-3		The drone's wing shall be capable of providing a climb rate of 2 m/s to an altitude of 500 m AGL	ConOps, RFP-MR27, Airfoil Shape	Hand Calculations	Wind tunnel testing	Concordia Hall Building	
	W-S-4		Wingspan shall not exceed 200 cm	Downsizing	N/A	N/A		
	W-W-1	Winglets	The wing shall have wingtip devices to improve drone efficiency by at least 20%	A-GEN-001, RFP-SP01, ConOps, RFP-MR28	CFD	Wind tunnel testing	Concordia Hall Building	Target value with OBJECTIVE to meet range requirement - optimal efficiency --> allows for less optimal propulsion methods & more buffer room for sub-optimal propulsion performance
	W-Al-1	Ailerons	Shall achieve a maximum deflection angle of 25 degrees or less	A-GEN-011 , Sadraey	CAD	Assembly	Aero Lab EV Building	To prevent flow separation which would reduce the aileron effectiveness. and reduce adverse effect on the stall angle, Sadraey p.668
	W-Al-2		Shall achieve a bank angle change of 30 degrees in 1.3 seconds or less at maximum deflection	A-GEN-011 , Sadraey	CFD, Wind Tunnel	X-plane	Aero Lab EV Building	Rationale: roll control depends on the mission profile, Sadraey p.12.12
	W-Al-3		The aileron shall be placed at more than 5% of the wing half-span away from the tip	A-GEN-011 , Sadraey	CAD	N/A		Rationale: to minimize the effect of tip vortices on the performance of the aileron, Sadraey p.669
Tail	T-D-1	Tail Design Operational Ceiling	The drone's tail design shall enable effective operation at altitudes of up to 4,000 meters ASL	S-TAIL-002, A-GEN-002, RFP-SP03	Hand Calculations	X-plane	Aero Lab EV Building	
	T-A-1	Tail Arm	The tail arm shall be long enough to provide static longitudinal stability with a static margin ranging from 5-15%	Sadraey,	Static Stability Analysis	Flight Test	TBD	Sadraey Ch.12
Ruddervator	Rd-1	Deflection Angle	Shall achieve a full deflection angle of at least 30 degrees	Sadraey	CAD	Assembly	Aero Lab EV Building	Pitch & Yaw control effectiveness Sadraey (Tables 12.3,12.12)
	Rd-2	Pitch Rate	Shall achieve a pitch rate of 20 degrees per second at a full deflection of 30 degrees	A-GEN-011, Sadraey	X-plane	Flight Test	TBD	
Landing Gear	LDG-1	Aircraft Stability	Aerodynamic loads on the landing gear design shall not induce a pitching moment that would destabilize the aircraft in flight	RFP-FC12	Dynamic Stability Analysis	X-plane	Aero Lab EV Building	Flight, gusts, wind (RFP)
Fuselage	FUSE-1	Size	The weight of the fuselage shall be carefully considered to ensure that there is sufficient weight allowance available for other components.	A-GEN-001 , RFP-SP01	CAD	Assembly	Aero Lab EV Building	Ensure all required components are self-contained within fuselage allowing for operational "functionality" as intended

B OML

The parts and assemblies delivered from the aerodynamics group have been summarized in Table B.1. The top level AERO node is as seen in the table below is a child node for the top level INTEGRATION node. This is to facilitate the flow of updates made to the OML by the AERO group to other team. The DMU is managed using GitHub and is setup and maintained by the aerodynamics team.

Table B.1: Part List for the OML DMU

Part Name	Part Number
Outer Mold Line Assembly	[A490-02-O-AERO-0001-C]
FUSELAGE	
Fuselage OML	[A490-02-O-AERO-0100-C]
WING	
Wing Assembly	[A490-02-O-AERO-0003-C]
Wing OML	[A490-02-O-AERO-0400-C]
Aileron - $\delta = 0$	[A490-02-O-AERO-0410-C]
Aileron - $\delta = -20$	[A490-02-O-AERO-0420-C]
Aileron - $\delta = 20$	[A490-02-O-AERO-0430-C]
EMPENNAGE	
Empennage Assembly	[A490-02-O-AERO-0002-C]
Inverted V Tail OML	[A490-02-O-AERO-0200-C]
Ruddervator - 0A - no deflection	[A490-02-O-AERO-0210-C]
Ruddervator - 1A - pitch down	[A490-02-O-AERO-0220-C]
Ruddervator - 1B - pitch up	[A490-02-O-AERO-0230-C]
Ruddervator - 2A - yaw left	[A490-02-O-AERO-0240-C]
Ruddervator - 2B - yaw right	[A490-02-O-AERO-0250-C]

The assembly can be accessed using the following link: [AERODYNAMICS DMU](#).

B.1 Wing Design

The benchmarking process facilitated a thorough comparison among diverse drone configurations, leveraging historical performance data as a reference (See Appendix A). An evaluation encompassing performance, manufacturability, and complexity criteria affirmed that the fixed-wing design represents the optimal configuration. Its flight performance characteristics closely align with the stipulated requirements in the RFP. Furthermore, this design extends benefits to other work packages due to its straightforward manufacturability and relatively low complexity in control systems compared to configurations involving motor rotations from vertical to horizontal and vice versa. The selection of this design is thus grounded in its alignment with performance objectives and its simplicity in manufacturability and control.

The accompanying XDSM illustrates the intricate relationships between design inputs and outputs, highlighting the iterative nature intrinsic to the design process. This visual depiction elucidates the interconnected aspects governing design evolution, offering insights into the dynamic nature of the overall design framework.

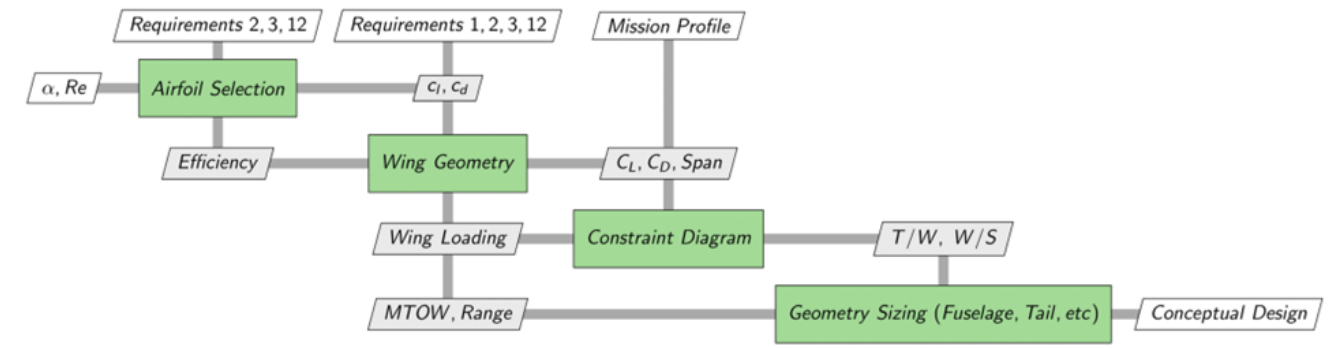


Figure: Design Structure Matrix (DSM) for development methodology.

Figure B.1: Design Structure Matrix

The airfoil selection is the first step. It must meet the maximum lift coefficient requirement imposed by [12] as well as meet the climb rate, operational altitude, and operational temperature requirements specified in the RFP. As previously mentioned in the requirements section (Section 1), the design must be operational even in the harshest conditions within the operational range to satisfy the aircraft-level ‘operational’ criteria.

For this reason, the Reynold’s number was calculated using extreme environmental conditions as specified in the RFP. The characteristic properties of the air were considered at the maximum altitude, at the lowest operational temperature. The speed was determined using RFP flight radius and flight time requirements. This in turn yielded a Reynold’s number of approximately 320,000. This is considered relatively low so the next step involved researching highly-cambered airfoil shapes as they yield relatively high lift at a “low” Reynold’s number.

Comparing the lift, drag, lift-to-drag graphs as a function of the angle of attack, it was determined that the FX 63-137 suited the operational conditions it would be subjected to while providing the most efficient aerodynamic properties.

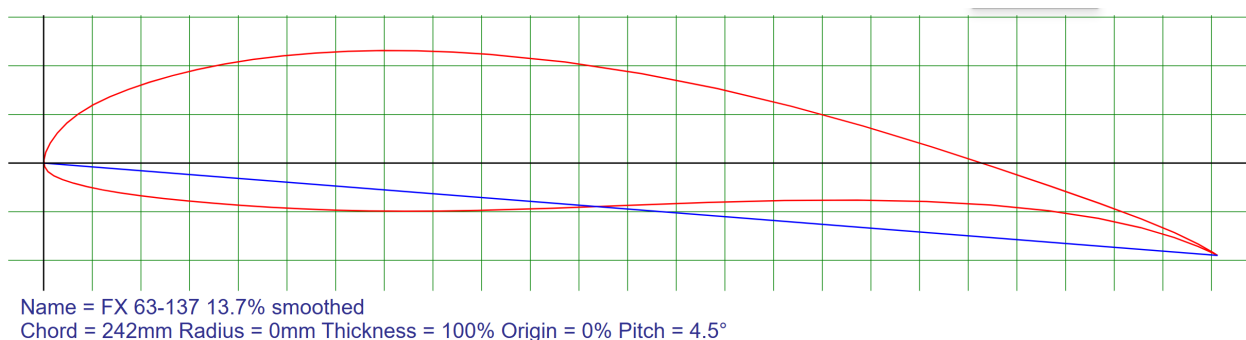


Figure B.2: Wing Airfoil - FX 63-137

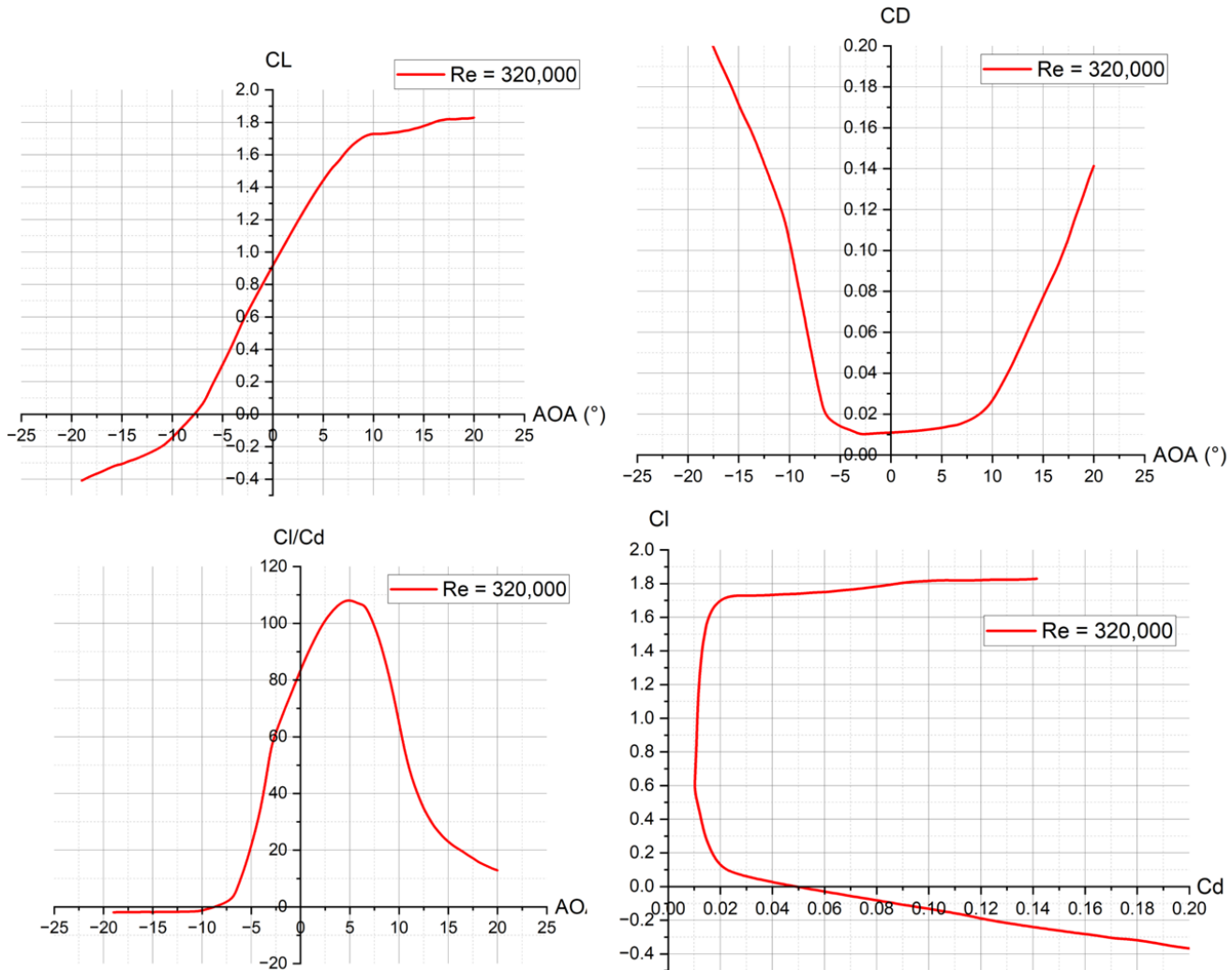


Figure B.3: FX 63-137 Aerodynamic vs. AOA

The FX 63-137 met the maximum lift coefficient requirement [12] while providing the greatest lift-to-drag ratio.

Now that the airfoil selection has been made, wing-geometry-specific requirements are taken as inputs alongside the lift and drag coefficients. Input wing requirements include maximum wingspan, freestream air velocity, environmental conditions defined at different pressure altitudes, and the MTOW.

It is important to note that due to manufacturability constraints of the wing and the lack of benefit provided by complexifying its geometry, the configuration selected has no taper, no sweep, no twist angle, and no dihedral angle.

The wing geometry is a straight wing with an airfoil of FX 63-137. Furthermore, at the start of the detailed design, the wingspan was recalculated using the programmed constraint diagram from the preliminary sizing phase. As one of the inputs of the constraint diagram program was the maximum takeoff weight (MTOW), entering the new MTOW generated the constraint diagram seen in below.

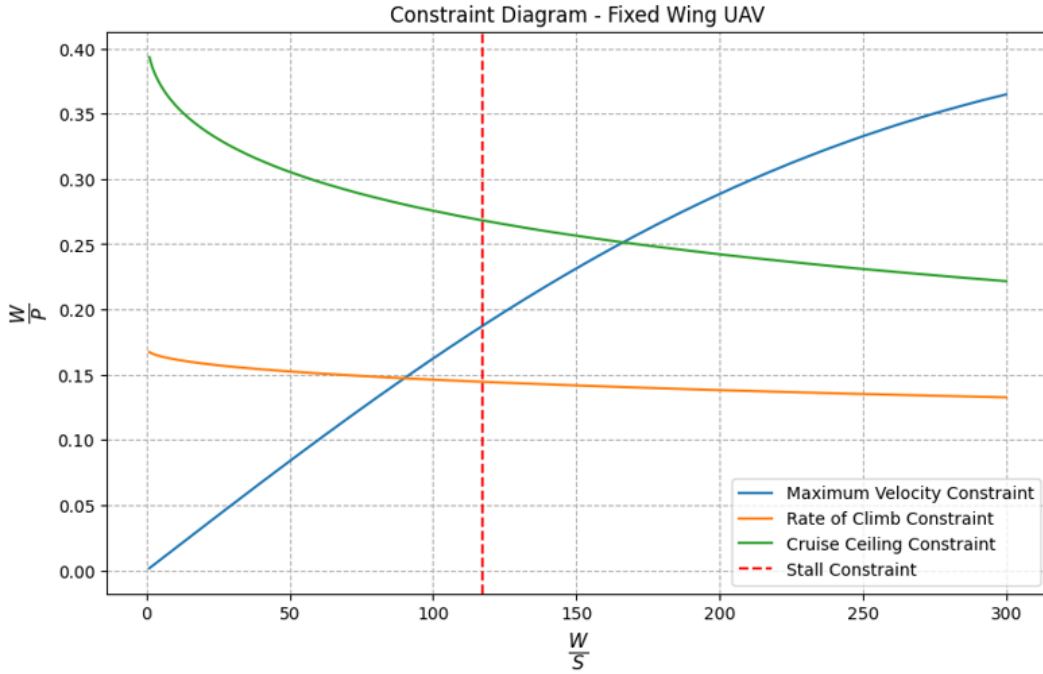


Figure B.4: Updated constraint diagram

The results from the final iteration of the constraint diagram were: The wingspan (b) = 2.94 m The wing loading $W/S = 151.26 \text{ N/m}^2$ and the power loading $P/W = 0.141$

B.2 Winglet Design

The winglets were added to the design to enhance aerodynamic performance and increase the range of the UAV. Winglet design and optimization is a long process and for the purpose of this project, existing studies and reports we used to design the winglet. Different parameters namely the height, blending radius, winglet airfoil, taper ratio and cant angle, were examined. Their effect on both L/D ratio and the stall behavior were studied. Once a design was decided based on a thorough literature review, the flow around the main wing (with winglets) was examined at cruise conditions, using CFD. Appendix D discuss the results and performance enhancements in detail.

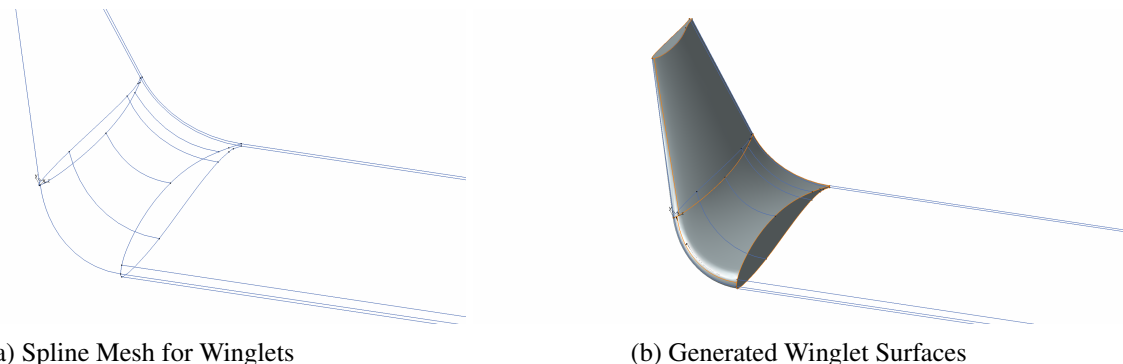
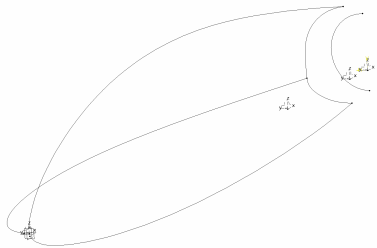


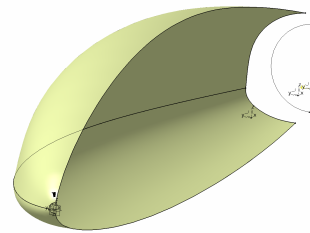
Figure B.5: Winglet Design Process

B.3 Fuselage Design

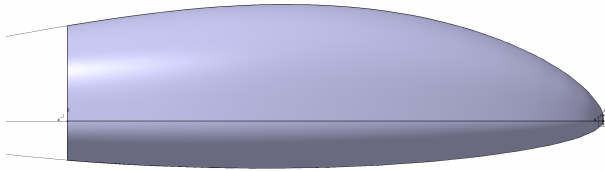
The design of the fuselage was iterative based on the fact that the airframe team decided to change the manufacturing method to 3D printing. This opened room for aerodynamics to chose a profile to minimize drag, yet be able to enclose all the components for the UAV. Hence, airfoils were chosen as means to design the UAV fuselage. Viewing the fuselage from the side, the airfoil profile is an FX 63-147 profile, as illustrated in Figure B.6c. Similarly, viewing the fuselage from the top as in Figure B.6d, is a NACA 0012 symmetric airfoil.



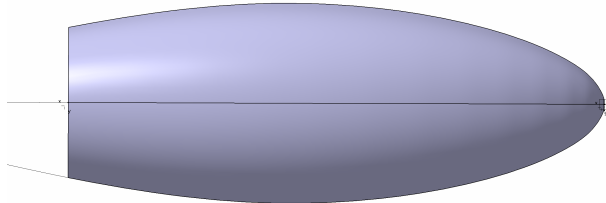
(a) Fuselage Guide Rail Splines



(b) Generated Surface Features



(c) Fuselage Side View



(d) Fuselage Top View

Figure B.6: Fuselage Design Process

B.4 Empennage Design

The major difference between wing design and tail design originates from the primary function of the tail. The primary function of the wing is to generate the maximum amount of lift, while the tail has two primary functions:

- Trim in both longitudinal and lateral directions
- Stability in both longitudinal and lateral directions
- Control in both longitudinal and lateral directions

During the preliminary design, the baseline design of the empennage was amended. The changes involved going from an H-tail to an inverted V-tail configuration. However, in terms of sizing, the design initially follows a traditional sizing, i.e., vertical stabilizer and horizontal stabilizer Figure B.7 depicts the process used to size the tail (horizontal stabilizer and vertical stabilizer) [12]

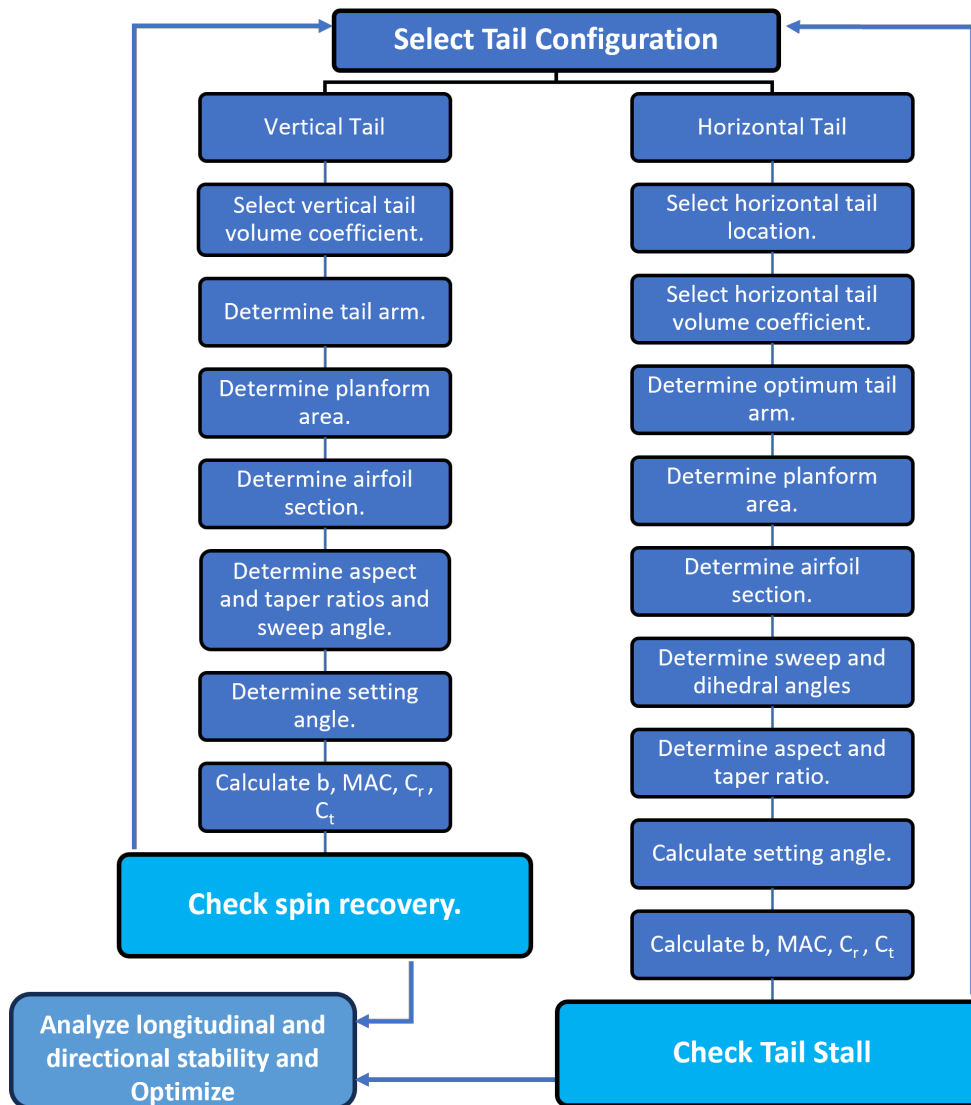


Figure B.7: Tail sizing methodology

The steps used to size the tail are detailed in this section:

- Select tail configuration.

Horizontal tail sizing:

1. Select horizontal tail location (aft or forward (canard)).
2. Select horizontal tail volume coefficient, V_H .
3. Calculate optimum tail moment arm (l_{opt}) to minimize the aircraft drag and weight.
4. Calculate horizontal tail planform area, S_h .
5. Calculate wing/fuselage aerodynamic pitching moment coefficient.
6. Calculate cruise lift coefficient, C_{Lc} .
7. Calculate horizontal tail desired lift coefficient at cruise from trim.

8. Select horizontal tail airfoil. Refer to the next subsection for details on this step
9. Select horizontal tail sweep angle and dihedral.
10. Select horizontal tail aspect ratio and taper ratio.
11. Determine horizontal tail lift curve slope, $C_{L\alpha_h}$.
12. Calculate horizontal tail angle of attack at cruise.
13. Determine downwash angle at the tail.
14. Calculate horizontal tail incidence angle, "i".
15. Calculate tail span, tail root chord, tail tip chord, and tail MAC.
16. Calculate horizontal tail generated lift coefficient at cruise (lifting line theory).
17. In script: If the horizontal tail generated lift coefficient is not equal to the horizontal tail required lift coefficient, adjust the tail incidence.
18. Check horizontal tail stall.
19. Calculate the horizontal tail contribution to the static longitudinal stability derivative ($C_{m\alpha}$). The value for the $C_{m\alpha}$ derivative must be negative to ensure a stabilizing contribution. If the design requirements are not satisfied, redesign the tail. Analyze the dynamic longitudinal stability. If the design requirements are not satisfied, redesign the tail.

Vertical tail sizing:

1. Select vertical tail configuration (e.g., conventional, twin vertical tail, vertical tail at swept wing tip, V-tail).
2. Select the vertical tail volume coefficient, V_V .
3. Assume the vertical tail moment arm (l_v) equal to the horizontal tail moment arm (l).
4. Calculate vertical tail planform area, S_v .
5. Select vertical tail airfoil section. Refer to the next subsection for details on this step
6. Select vertical tail aspect ratio, A_{rv} .
7. Select vertical tail taper ratio, λ_v .
8. Determine the vertical tail incidence angle.
9. Determine the vertical tail sweep angle.
10. Determine the vertical tail dihedral angle.
11. Calculate vertical tail span (b_v), root chord ($C_{v\text{root}}$), tip chord ($C_{v\text{tip}}$), and MAC_v.

V-tail sizing

Once the horizontal tail and vertical tail were sized, the V-tail was sized. Refer to the preliminary design report for detailed iterative calculations. In this section, the methodology used and the final dimension are presented

1. Calculate the total area required by adding the vertical and horizontal tail areas together[11].

2. Calculate the ideal dihedral angle for the inverted V-tail[9]:

$$\theta = \tan^{-1} \left(\sqrt{\frac{S_{vt}}{S_{ht}}} \right)$$

3. Introduce a flat section in the middle to enhance lift distribution and provide clearance between propellers; in this case, an 18 cm flat section was added.
4. Using geometrical projections, obtain the needed dimensions using the horizontal and vertical tail dimensions previously calculated.

Regarding the airfoil selection, a decision to change the tail airfoil (D002) from the original selection was made, as indicated on the project's decision log. In this section, the rationale behind this change is explained in detail and the new airfoil selection is presented.

Airfoil selection background

Tail requirement is that the horizontal tail must be clean of compressibility effect. In order for the tail to be beyond the compressibility effect, the tail lift coefficient is determined to be less than the wing lift coefficient. To ensure this requirement, the flow Mach number at the tail must be less than the flow Mach number at the wing. This objective will be realized by selecting a horizontal tail airfoil section to be thinner (say about 2 percent of MAC) than the wing airfoil section [12].

For instance, in example 6.2 of the book: It is discussed that “the horizontal tail airfoil section must have several properties. Two significant properties are: (i) symmetric and (ii) thinner than wing airfoil. The wing thickness-to-chord ratio is 12 percent. There are several airfoil sections that can satisfy these requirements, but we are looking for one with a low drag coefficient. A symmetric airfoil section with a minimum drag coefficient and 3 percent thinner than the wing airfoil section is NACA 0009.”[12].

From this, The wing is using the airfoil **WORTMANN FX 63-137 AIRFOIL** with $t/c_{max} = 13.7$. By the recommendations of the book, it was concluded that the airfoil to be used in the tail is **Selig S9032 (9%) symmetrical**.

$$t_{old} = t/c \times MAC_{tail} = 9\% \times (0.155 \text{ m}) = 0.01395 \text{ m} = 1.395 \text{ cm}$$

Ammendment

The airframe team expressed concerns regarding manufacturability because the tail section was too thin. Due to this concern, the airfoil selection was changed to a thicker airfoil, i.e., **NACA 0012** Whit a $t/c_{max} = 12\%$, which will result in a tail maximum thickness of:

$$t_{new} = t/c \times MAC_{tail} = 12\% \times (0.155 \text{ m}) = 0.0186 \text{ m} = 1.86 \text{ cm}$$

$$t_{increase} = 1.86 \text{ cm} - 1.395 \text{ cm} = 0.465 \text{ cm}$$

Final dimensions for the inverted V-tail

Table B.2: V-tail dimensions

	Dimension	Unit
Tail arm	0.886	m
Boom spacing	0.83	m
Tail half span	0.36	m
Tail chord	0.155	m
Incidence angle	27.3	°
Flat section	0.18	m

Table B.2 shows the final dimensions of the inverted V-tail.

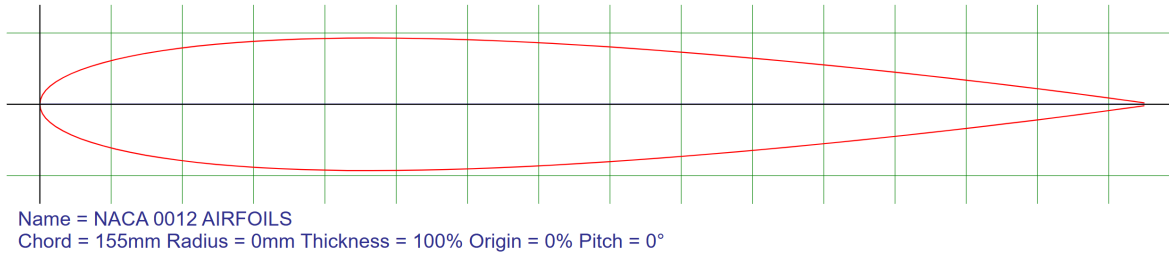


Figure B.8: Inverted V-Tail Airfoil - NACA 0012
[13]

Figure B.8 shows the final airfoil selected from the inverted V-tail empennage

B.5 Control Surface Design

B.5.1 Ailerons

Aileron Performance Evaluation In this report, the analytical procedure is compared to results obtained using computational fluid dynamics (CFD). To do so, the aircraft was modeled using CATIA, and ailerons were deflected at their maximum deflection angle of 20 degrees. The meshing was done using ANSYS Fluent Meshing, with settings that were common to all simulations. The meshing of the volume around the drone was done by simulating flow in a duct, with the duct size being proportional to the drone. The dimension of this duct is seen in the table below. The dimensions are made in terms of multiple lengths of the drone. For example, since the wingspan including the wing tips is 2.266 meters, the size of the box on either side of the wing tips should be as follows:

Total size of the duct in y = (size of the drone in y) + (y-min) X (size of the drone in y) + (y-max) X (size of the drone in y)

Total size of the duct in y = (2.226 m) + 2 X (2.226 m) + 2 X (2.226 m) = 11.13 meters

The size of the duct is represented in section D.2 and the settings used for the meshing are seen in section D.4. Below is the final aileron size and position:

- Span: 0.33877 m
- Chord: 0.06775 m
- Aileron start (distance from the x axis): 0.4658 m
- Aileron stop (distance from the x axis): 0.80457 m

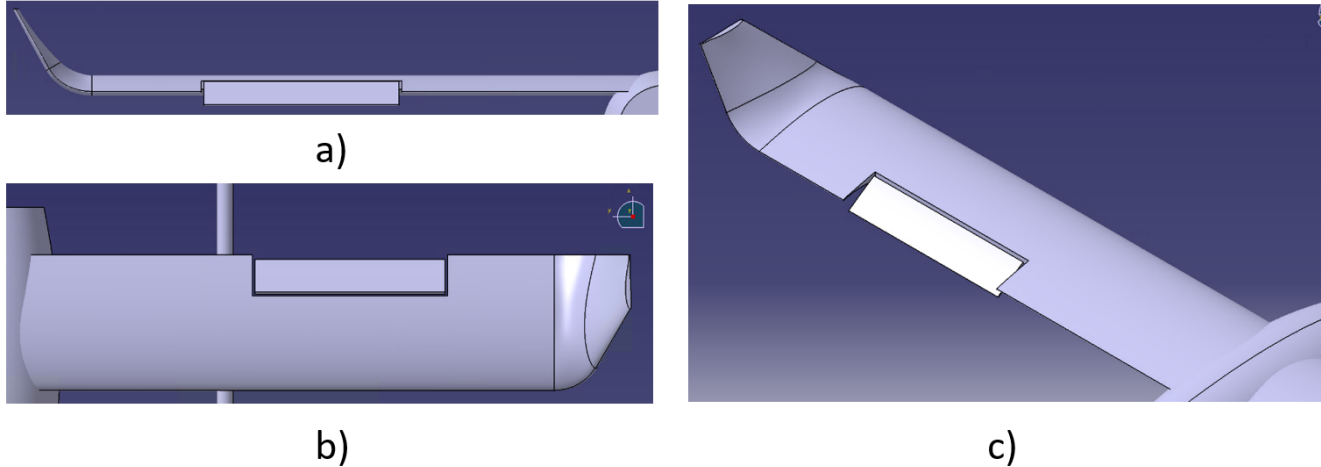


Figure B.9: Deflected Left Aileron seen a) from behind; b) from above; c) isometrically

That is the same dimension and position as the one seen in the preliminary design. After the increase of the wingspan from 1.7 m to 2 m, the airframe team indicated that the extra size between the ailerons and the winglets was needed due to the way it was going to be setup. The rib and foam setup at the wing tip is used to attach the winglets to the wing. Some space is needed for this setup to work, which is why the placement of the aileron stayed the same even after a wingspan increase. This decision should not have a negative impact on the performance of the ailerons, as they should still follow the requirements related to roll, as seen in the following pages. The sizing and the simulation settings mentioned yielded the following results, depending on the altitude (density) and the speed of the aircraft:

Table B.3: Comparison of Results from Hand-Calculations and CFD

Conditions	Hand-Calculations		CFD		Percent difference between CFD and hand-calculations
	Roll moment (Nm)	Time necessary to perform a 30-degree bank angle change (s)	Roll moment (Nm)	Time necessary to perform a 30-degree bank angle change (s)	
Case 1: 4000 m, 27 m/s	21.98	0.4082	20.92	0.4171	-4.82 %
Case 2: 4000 m, 22 m/s	14.59	0.48676	13.84	0.4979	-5.14 %
Case 3: 0 m, 27 m/s	32.86	0.3430	31.44	0.3496	-4.32 %
Case 4: 0 m, 47.35 m/s (estimated dive speed)	101.08	0.0046	97.22	0.0047	-3.82 %
4000 m, 22 m/s estimated from change in velocity	N/A	N/A	13.889	N/A	-4.80 %
0 m, 27 m/s estimated from change in density	N/A	N/A	31.275	N/A	-4.82 %

In the first case, the altitude is the ceiling altitude, determined to be 4000 m from the mission profile. The speed is 27 m/s determined to be the cruise velocity. This makes case 1 to represent the minimum aircraft roll moment at cruise conditions. The absolute minimum roll moment is achieved when loitering or approach phase of flight, due to the smaller velocity. However, that velocity was not determined by the integration team at the time of writing this report, so an arbitrary velocity of 22 m/s was chosen instead for case 2. Case 3 is at cruise speed but at sea level density. The fourth and final simulation was made for the sole purpose of determining the maximum hinge moment the aileron can have.

These three simulations also aim to confirm that the hand calculations made were correct. According to the theory, the aircraft roll moment is supposed to be proportional to the density and to the velocity squared. Based

on the numbers from the first case, we can estimate what should be the values for the second and third cases. For example, $27/22 = 0.8148$ so the new roll moment should be:

$$M_{new} = M_{old} \times 0.8148^2 = 20.92 \text{ Nm} \times 0.8148^2 = 13.889 \text{ Nm}$$

The same procedure can be done for the change in density as well, yielding a moment of 31.275 Nm for a density at sea level. This can be seen in the last two rows of the table above. There is approximately a 0.5 percent difference from the roll moment found with this method, and the one from CFD. Thus, it confirms the relationship between the roll moment, the density, and velocity.

The difference between CFD and analytical results are all similar, with a percent difference ranging from -3.82 to -5.14 percent between the two methods. The lower roll moment seen in CFD is because of the more complex and accurate equations compared to those used for the hand-calculations.

The best way of determining the time needed for a 30-degree bank angle change for CFD would be a transient simulation. Unfortunately, these simulations were not possible due to computational limitations. For it to be possible to compute in less than 24 hours, either the residuals would not be made stable for each time step, or the cell size would be too big. Either way, it would be unlikely that the result of such a simulation would be more accurate than the analytical method. From the simulations done so far, about 300-400 iterations are required to get to a stable solution where the residuals stay constant. With a time-step of 0.01 seconds, and 300 iterations per time-step, it becomes impossible to arrive at an accurate transient solution in a reasonable time.

This is why this requirement will only be verified in the wind tunnel. In the roll moment table seen above, the bank angle change for CFD was calculated the same way as for the hand-calculation method. Only difference is that it uses a different roll moment to do the calculations.

Other simulations were made to determine more characteristics of the aileron performance. These simulations were made with the old configuration of the aircraft, where the wing size was 1.7 m, and the fuselage was at a slightly different position. Those results can be seen below.

Table B.4: Results of CFD simulations made with the old configuration

Case Number	Case Description	Min cell size (mm)	Max Cell Size (mm)	Total Cells	Roll Moment (Nm)	Yaw Moment (Nm)	Pitch Moment (Nm)	Lift (N)	Drag (N)
1	Ailerons 0 AOA	0.9	200	4,461,619	-9.86	0.29	3.02	32.00	9.10
2	Ailerons 14 AOA	0.9	200	4,533,968	-9.93	2.24	-5.11	122.47	22.29
3	Ailerons inclined on the other side	0.9	200	4,449,603	9.87	-0.46	3.04	31.94	8.99
4	Ailerons no booms or landing gear	0.9	200	3,718,875	-9.95	0.43	3.25	32.32	5.70
5	Ailerons at sea level	0.9	200	4,461,619	-14.41	0.49	4.60	47.41	12.87

These results have helped confirm assumptions on the performance of the ailerons. Case 2 was made to determine the effect of the angle of attack on the roll moment. It resulted in an increase in roll moment of 0.71 percent, meaning that the performance of the ailerons is not overly impacted by the angle of attack. In case 3, the ailerons are inclined on the opposite side. The magnitude of roll moment is increased by only 0.1 percent, indicating that simulation made in case 1 is precise enough. In case 4, it is confirmed that the presence of booms only minimally affects the performance of the ailerons, as the roll moment is increased only by 0.9 percent. With the old configuration, we see the same principle as with the new one, where the density is directly proportional to the roll moment.

Overall, the requirement on the time needed to make a bank angle change should be respected. The values obtained range between 0.3430 s and 0.4979 s for conditions within the mission profile. This is below the requirement of 1.3 seconds, even when considering a safety factor of 2. Therefore, the performance of the aileron is sufficient to control the aircraft roll. The size and the placement of the aileron can stay intact.

Hinge Moment Calculation To determine the maximum hinge moment that the aileron actuator would need to deploy when extended to its maximum deflection of 20 degrees, the simulation at sea level density and 47.35 m/s speed was used. That is the estimated velocity for diving, provided by integration. Lift and drag forces acting on the aileron were compiled. They were used to calculate the hinge moment using the same technique as the one used by the C&C team. Here are the steps used to calculate the maximum required servo torque:

1. Aileron selection: The left aileron is inclined down by 20 degrees, the maximum deflection angle. The aerodynamic force is always higher on the aileron that is inclined downwards.
2. Drag force acting on the right aileron: $D = 11.60 \text{ N}$
3. Lift force acting on the right aileron: $L = 23.54 \text{ N}$
4. Force acting normal to the right aileron surface: $F_n = L \times \cos(20) + D \times \sin(20) = 23.54\cos(20) + 11.60\sin(20) = 26.09 \text{ N}$.
5. Required torque: $T = \text{force} \times \text{aileron half-chord} = 26.09 \text{ N} \times 0.5 \times 0.06775 \text{ m} = 0.8837 \text{ Nm}$
6. Required servomotor torque: $T_{\text{servo}} = \text{required torque} \text{ Nm} \times 10.2 \text{ Kg; cm N}^{-1} \times \text{m}^{-1} = 9.01 \text{ kg - cm}$

This procedure can also be done for other situations. The situation that yields the highest forces, but could still be in the mission profile is the aircraft at sea level traveling at 27 m/s. The maximum forces obtained from this situation are $D = 4.21 \text{ N}$ and $L = 8.32 \text{ N}$ which yield a maximum torque of 3.1989 kg-cm . That torque is below the maximum actuator torque of 13.06 kg-s .[6]. Even with the safety factor of two that C&C recommended, the actuator can still operate under those conditions.

However, at dive conditions, the hinge moment that occurs is 9.01 kg-cm . With a safety factor of 2, this becomes 18.02 kg-cm , which yields a maximum safety factor of 1.44. This safety factor should still be sufficient because the ailerons are not necessarily used to their maximum deflection angle in dive conditions. However, it is still something that will be monitored in collaboration with C&C.

The maximum possible aerodynamic forces acting on the aileron is $D = 11.60 \text{ N}$ and $L = 23.54 \text{ N}$, which makes for a total maximum force of 26.24 N acting on the aileron. According to the Airframes 1 team, this number is realistic for the aileron. Although they would need to do more simulations and testing to be sure, the ailerons should be able to resist such a load.

B.5.2 Ruddervators

In the pursuit of optimizing drone design, an extensive examination of ruddervator sizing methodologies was undertaken. The team decided to leverage the data featured in the State of the Art, exclusively for drones with the same similar characteristics. This included analysis of the drones' —CW-25E, Great Shark F320, and V500E—average ratios for ruddervator chord to empennage chord and ruddervator span to empennage span. The results yielded ruddervator chord to empennage chord of approximately 40 percent and ruddervator span to empennage span of approximately 80 percent. These ratios were then applied to the dimensions of the empennage. Which resulted in specific dimensions of 61.43 mm for the ruddervator chord and 290.45 mm for the span. Finally, CFD analysis was done for three critical maneuvers, pitch up, pitch down, and yaw right. The result and analysis can be found in section D.5.3

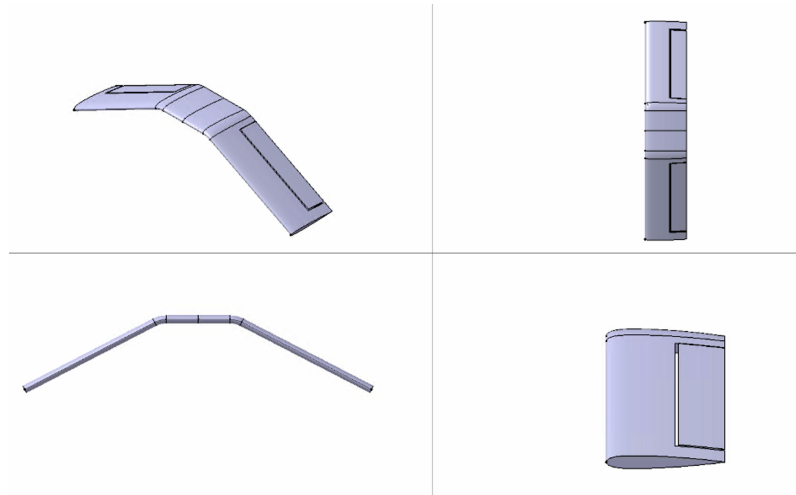


Figure B.10: Empennage with Ruddervator Model

B.6 Fairings, Blisters and Openings

This section discusses the effect of any openings of objects protruding outside the OML on the performance of the aircraft.

Fairings The only critical objects that were brought to attention to the aero group were the servos commissioned to operate the ruddervators on the tail. This was because the tail is very thin and there is no space to put the servos inside. A preliminary CFD analysis (without mesh independence study), showed that there is no critical lift penalty due to the presence of the servo and adding a fairing to reduce drag would not change the flow disturbance around that part drastically. Hence, the aero group opted not to have a fairing around the mentioned servo.

Openings Due to the overheating of the internal components, it was important to introduce an opening in the front of the aircraft. An analysis performed on the UAV showed that there were no effects in terms of lift reduction. However, it was suspected that there would be a drag penalty due to this opening. The drag analysis was performed by the propulsion team.

C Performance and Load Analysis

C.1 Stability

The following subsections present the detailed static and dynamic stability analysis.

C.1.1 Static Stability

In order to have an stable configuration it is desired that the center of gravity (CG) stays in front of the neutral point (NP) at all times. The plot of the pitching moment (C_m) should have an overall negative slope at any angle of attack (AOA) which indicates stability. Furthermore, at the balance angle $C_m=0$ there must be positive lift in order for the aircraft to fly. The overall negative slope of the pitching moment coefficient (C_m) versus the angle of attack (AOA) is a key indicator of static stability for an aircraft. This negative slope contributes to the stability of the aircraft's pitch. Following the main reason behind a negative slope are indicated:

1. Restoring Force:

A negative slope of C_m versus AOA implies that as the angle of attack increases (nose-up attitude), the pitching moment acts in the opposite direction, providing a restoring force. This restoring force helps bring the aircraft back to its original, trimmed position after a disturbance, such as a gust or a control input[12].

2. Stable Equilibrium:

In a stable equilibrium, when the aircraft experiences a perturbation (change from its trimmed state), the negative slope ensures that the restoring moment tends to return the aircraft to its original attitude. This characteristic is crucial for maintaining a stable and level flight.

3. Pilot Control:

A negative slope makes the aircraft more controllable for the pilot. It means that the aircraft naturally resists excessive changes in pitch, providing a predictable and manageable response to control inputs.

4. Damping Effect:

The negative slope contributes to the damping effect in pitch. Damping is important for preventing oscillations or divergent behavior in the aircraft's response to disturbances.

Static stability evaluation procedure

The following steps have been made using the software XFLR5

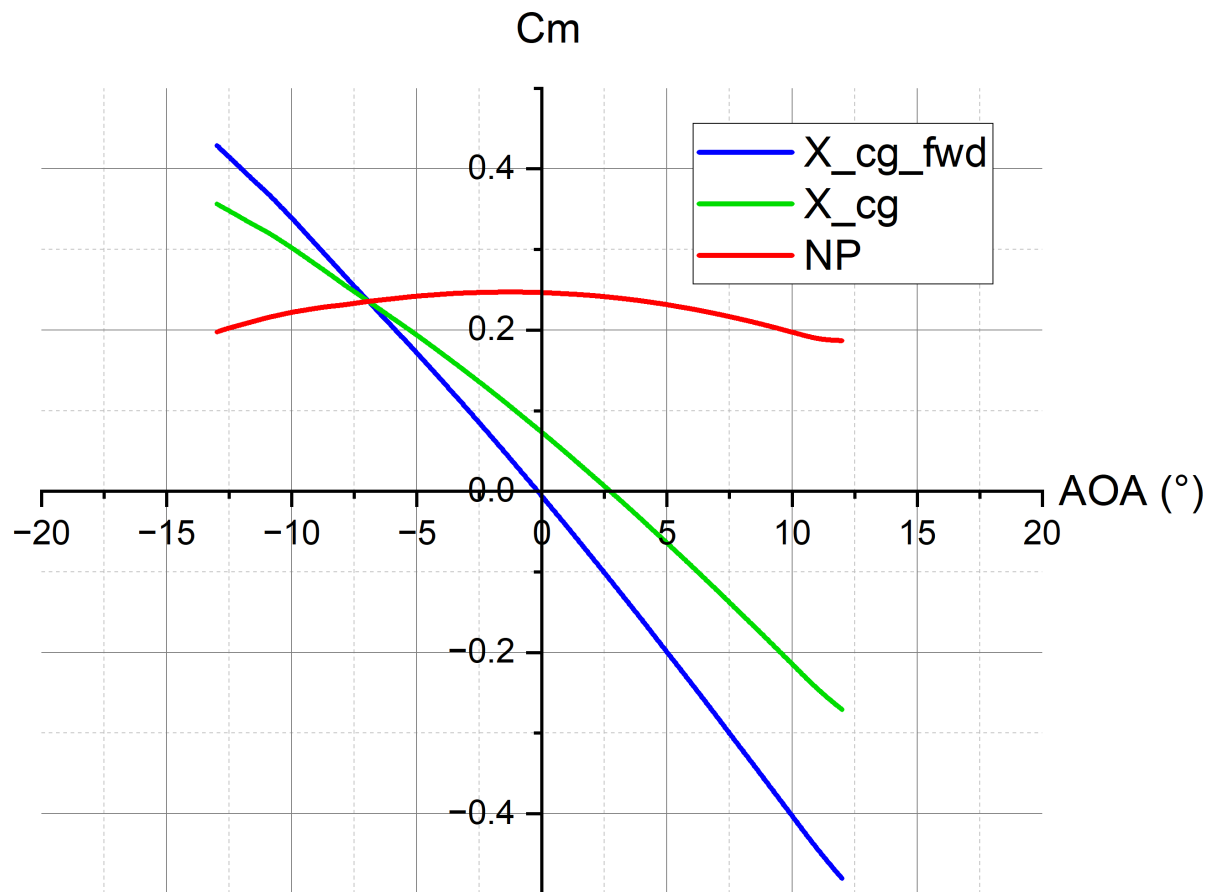
1. Define multiple locations along the MAC to place the total mass of the aircraft.

$$X_{cg} = \frac{c}{4_{wing}} + \Delta \left(\frac{c}{4_{Tail}} \right)$$

2. By trial and error, find the neutral point (red curve on Figure C.1).

3. By trial and error, find the forward CG limit, i.e., before the curve passes the first quadrant into the second and third (blue curve)Figure C.1.

4. Achieve a satisfactory static margin. In this case the target static margin was 0.12. Then locate the Center of Gravity (Green line)Figure C.1.

Figure C.1: C_m vs AOA plot

Static stability results

Table C.1: Static stability results

Parameter	Distance [m]
X_{CoG}	0.460
Y_{CoG}	0.315
Z_{CoG}	0.386
$X_{CpAOA} = 0$	0.398
X_{NP}	0.488
SM	0.120

Table C.2: Aircraft's moment of inertia

Moment of Inertia	Kgm ²
I _{xx}	0.48
I _{yy}	1.07
I _{zz}	1.45
I _{xz}	0.14

$$X_{CP} = 0.08 \text{ m from the leading edge} = 33\% \text{ of the MAC}$$

$$X_{NP} = 0.173 \text{ m from the leading edge} = 71\% \text{ of the MAC}$$

$$X_{CG} = 0.144 \text{ m from the leading edge} = 59\% \text{ of the MAC}$$

$$X_{CG_FWD} = 0.09 \text{ m from the leading edge} = 37\% \text{ of the MAC}$$

$$SM = \frac{X_{NP} - X_{CG}}{MAC_w} = \frac{0.173 - 0.144}{0.2242} = 0.12$$

The positive static margin (SM) is synonymous with stability. As specified in the sub-requirement T-A-1, between 5% and 15% of the MAC was acceptable; therefore, this requirement has been satisfied

C.1.2 Dynamic Stability

First, consider the definition of stability: Flight stability is defined as the inherent tendency of an aircraft to oppose any input and return to the original trim condition if disturbed [12].

In order to ensure an stable dynamic behavior, 2 longitudinal modes and 3 lateral modes were analyzed using the software xfri5.

Dynamic Longitudinal Stability

Longitudinal stability refers to the aircraft's inclination to revert to its original longitudinal equilibrium state, characterized by parameters like the steady-state angle of attack and forward speed, following a disturbance caused by a longitudinal factor such as a vertical gust. [12]. Concerning dynamic longitudinal stability, the analysis involves investigating how an aircraft reacts to a disturbance in the longitudinal direction. Specifically, it examines how a longitudinally dynamically stable aircraft responds when subjected to a vertical gust[12].

The maneuvers studied were:

1. Short period Phugoid mode
2. Long period Phugoid mode

Table C.3 shows the level of acceptability for the pilot, where 1 is very comfortable, 2 is hardly comfortable, and 3 is uncomfortable.Daming ratio is used to evaluate this maneuver

Table C.3: Phugoid Mode Requirements [12].

Level of Acceptability	Requirement
1	Damping ratio of phugoid mode (ζ_{ph}) ≥ 0.04
2	Damping ratio of phugoid mode (ζ_{ph}) ≥ 0.0
3	Time to double the amplitude at least 55 seconds

Dynamic Lateral Stability

When an aircraft with lateral-directional dynamic stability encounters a disturbance in the lateral-directional axis (such as a horizontal gust impacting the vertical tail), the aircraft will counteract the disturbance and ultimately revert to its initial trim state[12].The analysis of dynamic lateral-directional stability involves examining how an aircraft responds to disturbances in the lateral-directional axis. In a typical aircraft, this response manifests as a second-order oscillatory mode, commonly referred to as Dutch roll, alongside two first-order modes known as spiral and roll[12].

Summarizing, the maneuvers studied for dynamic lateral stability were:

1. Roll subsidence mode
2. Dutch roll oscillation mode

3. Spiral mode

Roll mode analysis

Table C.4 shows the level of acceptability for the pilot where 1 is very comfortable, 2 is hardly comfortable and 3 is uncomfortable. Time constant is used to evaluate this maneuver. Named as such, the roll mode signifies a rotation around the x-axis, inducing a shift in the bank angle. In essence, the roll mode or roll subsidence mode is a first-order reaction marked by a specific time constant. To ensure satisfactory lateral-directional handling qualities in an aircraft, it is necessary for the roll time constant (T_r) of the roll subsidence mode to fall below the specified values outlined in the table C.4.

Table C.4: Roll Mode Time Constant Specification (Maximum Value)[12]

Flight phase	Aircraft class	Tr		
		Level 1	Level 2	Level 3
A	I, IV	1	1.4	10
	II, III	1.4	3	10
B	All	1.4	3	10
C	I, IV	1	1.4	10
	II, III	1.4	3	10

Spiral mode analysis

The spiral mode, responding to lateral-directional disturbances, involves a first-order reaction characterized by a time constant, manifesting as a yawing motion around the z-axis with a change in yaw angle. In conventional aircraft, the spiral mode is often inherently unstable, and specific stability requirements are typically not imposed. Permissible light instability is allowed, but restrictions are placed on the minimum time for the mode to double its amplitude, known as allowable divergence [12]. To meet handling quality standards, an acceptable spiral mode assumes the aircraft is trimmed for straight and level flight with no bank angle, yaw rate, and free cockpit controls. The specification focuses on the time it takes for the bank angle to double following an initial disturbance (up to 20 degrees), with prescribed minimum times outlined in table C.5, which influences aileron design requirements [12].

Table C.5: Time to double amplitude in spiral mode [12]

Aircraft class	Flight phase	Minimum time to double amplitude in spiral mode		
		Level 1	Level 2	Level 3
I, IV	A	12	8	4
	B and C	20	8	4
II, III	A, B, C	20	8	4

Dutch roll analysis

The response known as Dutch roll, a second-order phenomenon, is defined by both a damping ratio (d) and an oscillation frequency (d). Table C.6 outlines the specified criteria for crucial dutch-roll parameters, including the damping ratio and dutch-roll frequency. It is imperative that both the frequency and damping ratio of the dutch-roll mode surpasses the prescribed values detailed in Table C.6.

Table C.6: Dutch-Roll Mode Handling Qualities [12]

Level	Flight Phase	Aircraft Class	ζ_d	$\zeta_d \omega_{nd}$ (rad/s)	ω_{nd} (rad/s)
1	A	I, IV	0.19	0.35	1.0
1	II, III	All	0.19	0.35	0.4
1	B	All	0.08	0.15	0.4
1	C	I, II, IV	0.08	0.15	1.0
1	III	All	0.08	0.15	0.4
2	All	All	0.02	0.05	0.4
3	All	All	0.02	No limit	0.4

Using XFLR5 software, the following results were obtained. Table C.7 summarizes the results obtained from testing the aircraft under the 5 modes.

Table C.7: Dynamic Stability Characteristics

Maneuver	Real	Imaginary	ζ	ω_d	ω_n	T_r	t_2
Short period Phugoid	-2.170	± 3.80	0.496	0.605	0.697	-	-
Long period Phugoid	0.009	± 0.77	0.013	0.124	0.124	-	-
Roll	-6.800	0	-	-	-	0.147	0.102
Dutch roll	-1.020	± 1.72	0.502	0.278	0.322	-	-
Spiral	0.577	0.000	-	-	-	-	12.010

Conclusion

The unmmanned UAV lies under category (II) homebuilt. With this consideration, we can compare the results in table C.7 to the tables above described

1. Short period Phugoid mode: $\zeta_{ph} = 0.496$. Therefore, the level of acceptance is 1. Meaning the airplane is stable in this maneuver, and the pilot would be very comfortable with this perturbation.
2. Long period Phugoid mode: $\zeta_{ph} = 0.013$. Therefore, the level of acceptance is 2. Meaning the airplane is stable in this maneuver, but the pilot would be hardly comfortable with this perturbation.
3. Roll subsidence mode: $T_r = 0.147$. This value is less than 1 and 1.4 at every flight phase. So, the level of acceptance is 1. Meaning the airplane is stable in this maneuver and the pilot would be very comfortable with this perturbation.
4. Dutch roll oscillation mode: $\zeta_d = 0.502$. This value is more than 0.19 and 0.08 at every flight phase. Therefore, the level of acceptance is 1. Similarly, $\zeta_d * \omega_{nd} = 0.16$. This value is bigger than 0.15 but less than 0.35. Therefore, the overall level of acceptance is 2. Meaning the airplane is stable in this maneuver, but the pilot would be hardly comfortable with this perturbation.
5. Spiral mode: $t_2 = 12.01$ s which lies on level 2 of acceptability. Meaning the time to double amplitude is acceptable. Thus, no correction to the V-tail is needed because the Pixhawk autopilot should be able to correct this perturbation.

Figure C.2 and Figure C.3 show the complex plane representation graphs of the 5 different perturbation modes.

Lateral modes

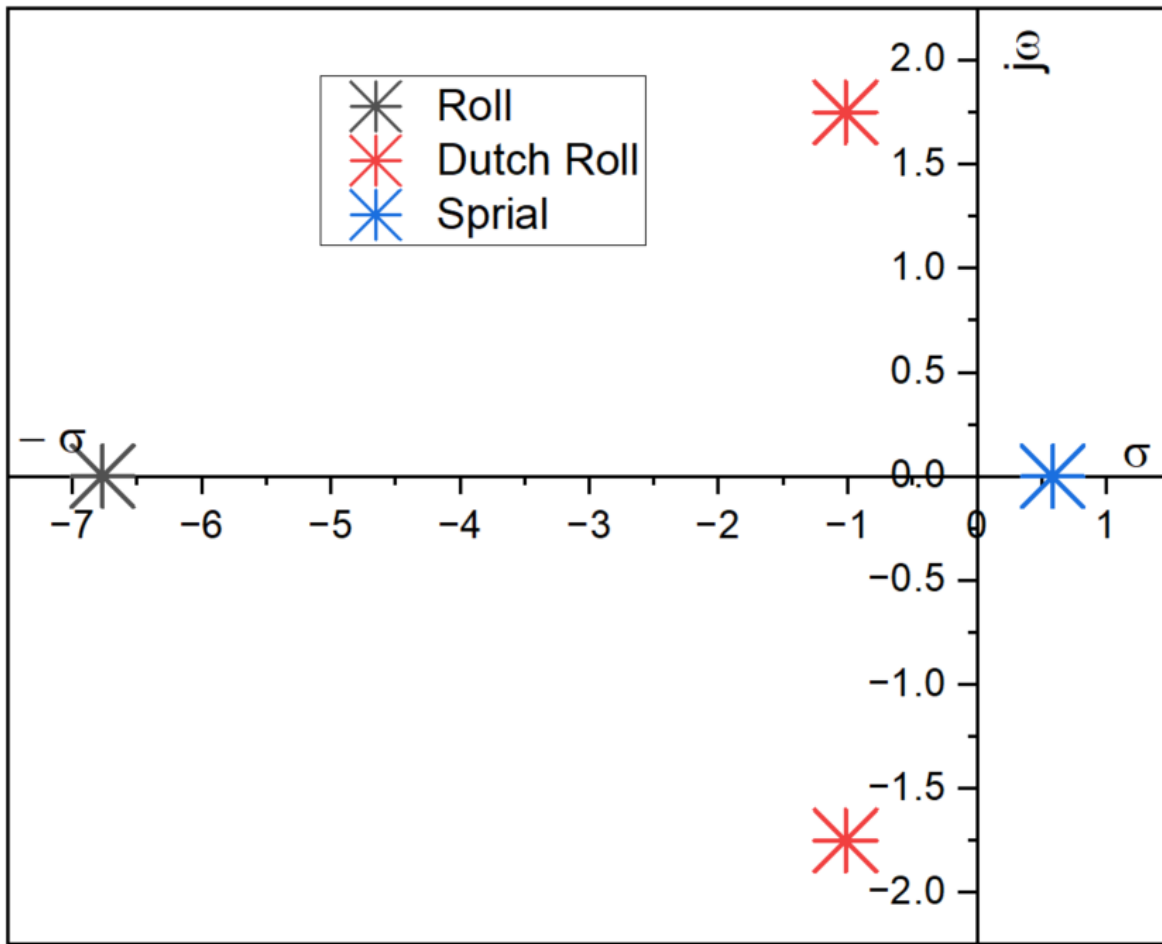


Figure C.2: Complex plane for lateral modes

Longitudinal modes

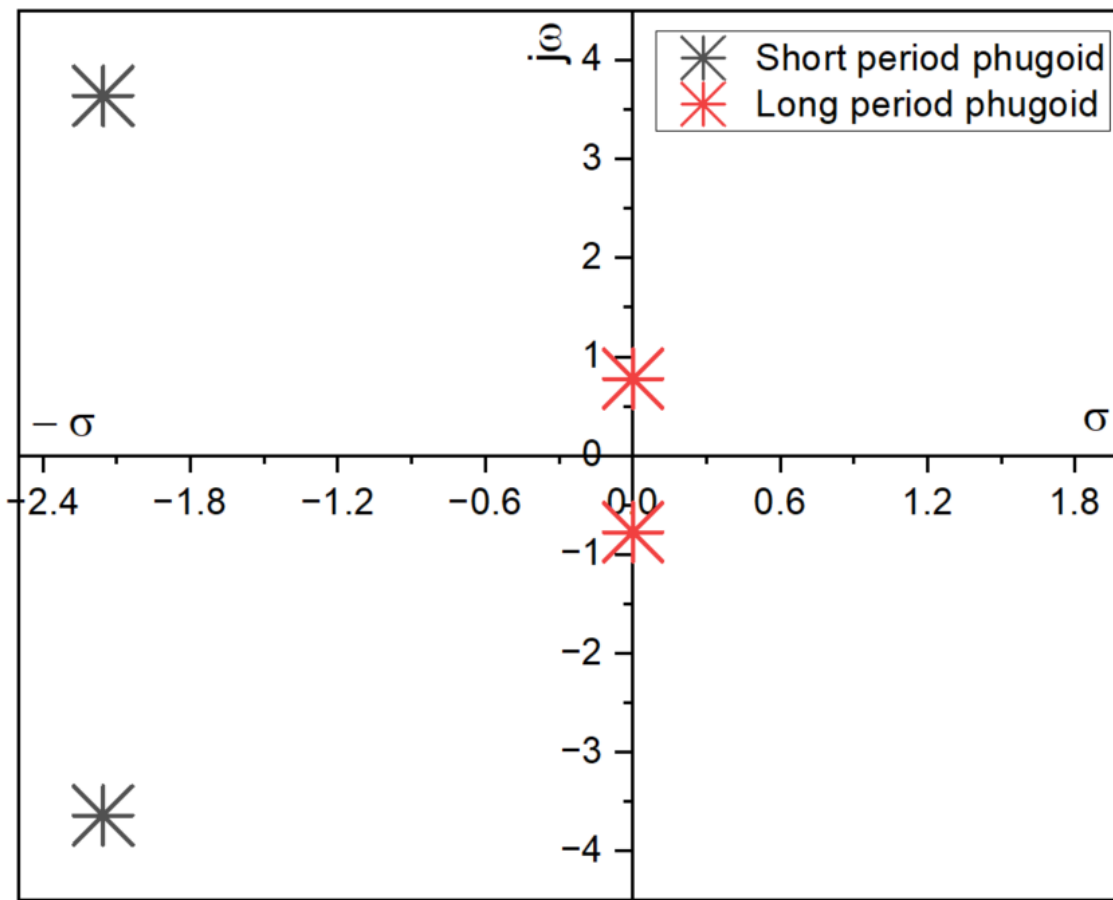


Figure C.3: Complex plane for longitudinal modes

D Computational Fluid Dynamics

The OML model prepared by the aero group was used for all the CFD analysis. The design was updated several times until the external geometry was established in its final form. The following subsections discuss the process of computational fluid dynamics for the project and the results are presented in subsection D.5.

NOTE: The process and results are presented for the final geometry and setup. Older cases were discarded and hence, have not been presented.

D.1 Geometry for CFD

An important aspect of setting up CFD is to have a geometry with simplified features. Excessive features can lead to slow processing times, and inaccurate results in many cases.

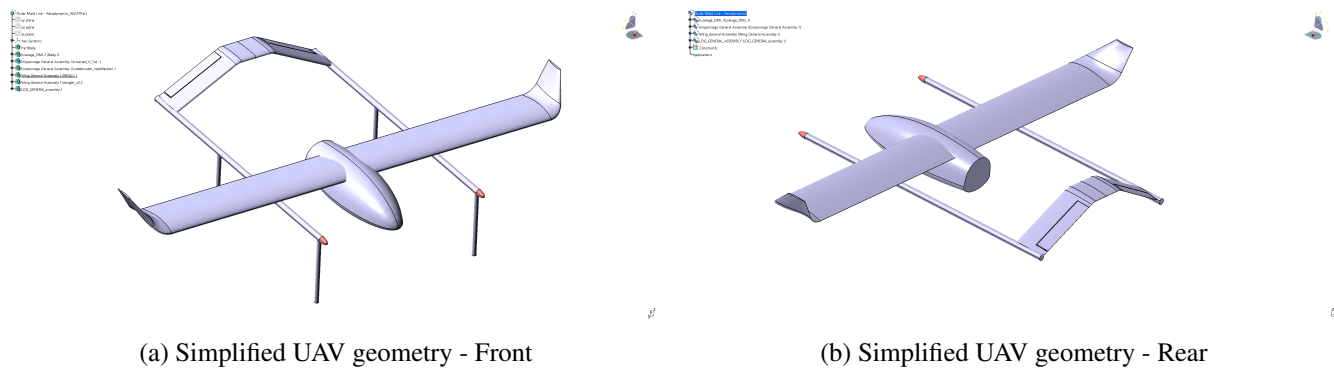


Figure D.1: Simplified Geometry for CFD

D.2 Domain Geometry

The domain of the flow was established based on review literature and past experience. In addition to that, different geometries were tested with the same mesh settings in order to see any change in results. Figure D.2 shows the finalized flow domain selected for all the simulation cases.

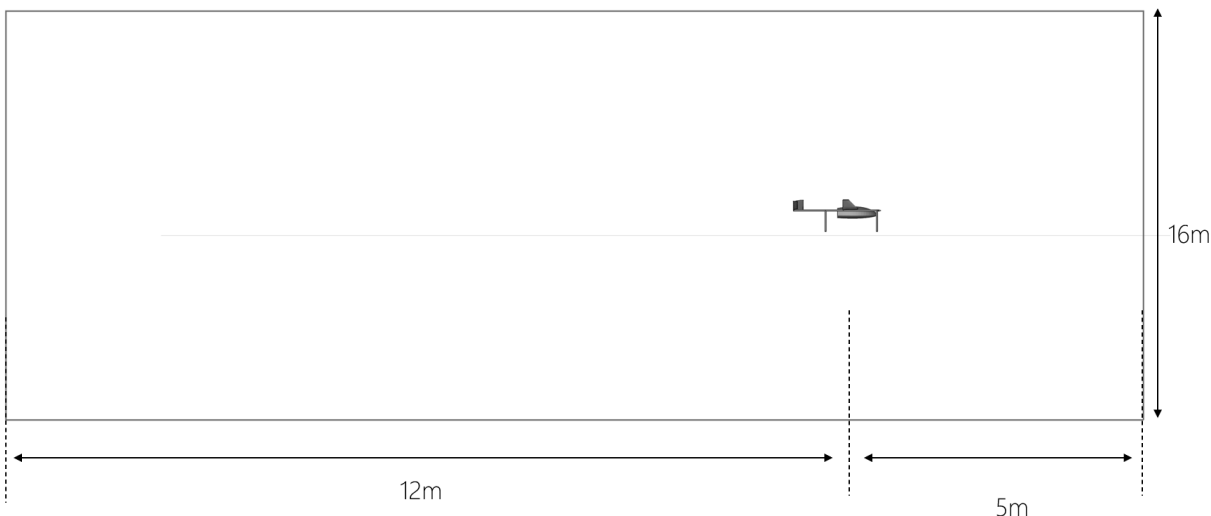


Figure D.2: Flow Geometry Domain - (not to scale).

D.3 Mesh Independence Study

An extensive mesh independence study was carried out to reduce the risk of having inaccuracies in results across all the simulations being run. The outcome of the mesh independence study was to have a standardized mesh setting, mesh creation workflow and flow domain size across all the simulations being run by the aero group. Table D.1 summarizes results obtained from the mesh independence of a model selected for the mesh independence study.

Table D.1: Mesh Independence Study Results

Case Number	Min cell size (mm)	Max Cell Size (mm)	Total Cells	Lift (N)
1		2	400	1,965,566
2		1.8	400	2,615,434
3		0.9	300	3,718,875
4		0.9	250	4,009,485
5		0.9	200	4,461,619
6		0.675	150	7,299,864
7		0.45	100	15,221,888

As can be seen from Figure D.3, the results start to converge after a cell count of approximately 6 million cells. Hence, the mesh settings of *Case 5* from Table D.1 were chosen for all the simulations to be run by the aero team.

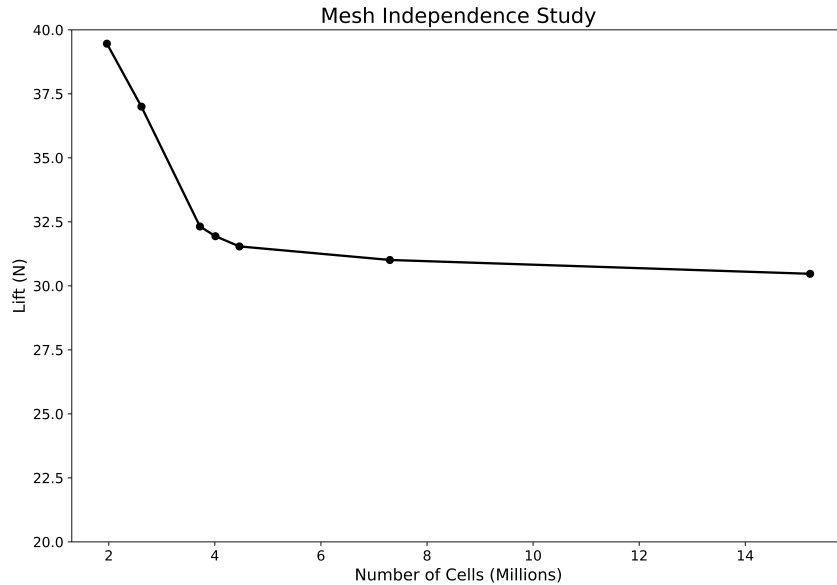


Figure D.3: Mesh Independence Study Plot

D.4 Meshing Strategies

Following the discussion in subsection D.3, a common meshing size and strategy was established for the aerodynamics group in order to be consistent while collecting all the data. The final mesh settings are presented in Table D.2.

Table D.2: Final Mesh Settings and Setup

Aircraft General Mesh			
Aircraft Surface		Fluid Domain Surface	
Minimum Cell Size	Maximum Cell Size	Minimum Cell Size	Maximum Cell Size
1 mm	4 mm	4 mm	100 mm
Boundary Layers			
Type	Number of Layers	Minimum Cell Size	Growth Rate
Uniform	6	0.9 mm	1.1

By using the settings presented in Table D.2, the following strategy is used to create mesh:

1. The domain is defines as shown in Figure D.2.
2. Surface mesh is defined using the appropriate setting for the aircraft surface as well as the domain.
3. Boundary layers are added to the model.
4. A volume mesh is created using the surface mesh and boundary layer settings.

This procedure was consistently used across all the cases to have consistency in results obtained. Figure D.4a, D.4b and D.4c show the surface mesh for different aircraft components and Figure D.4d shows the added volume mesh.

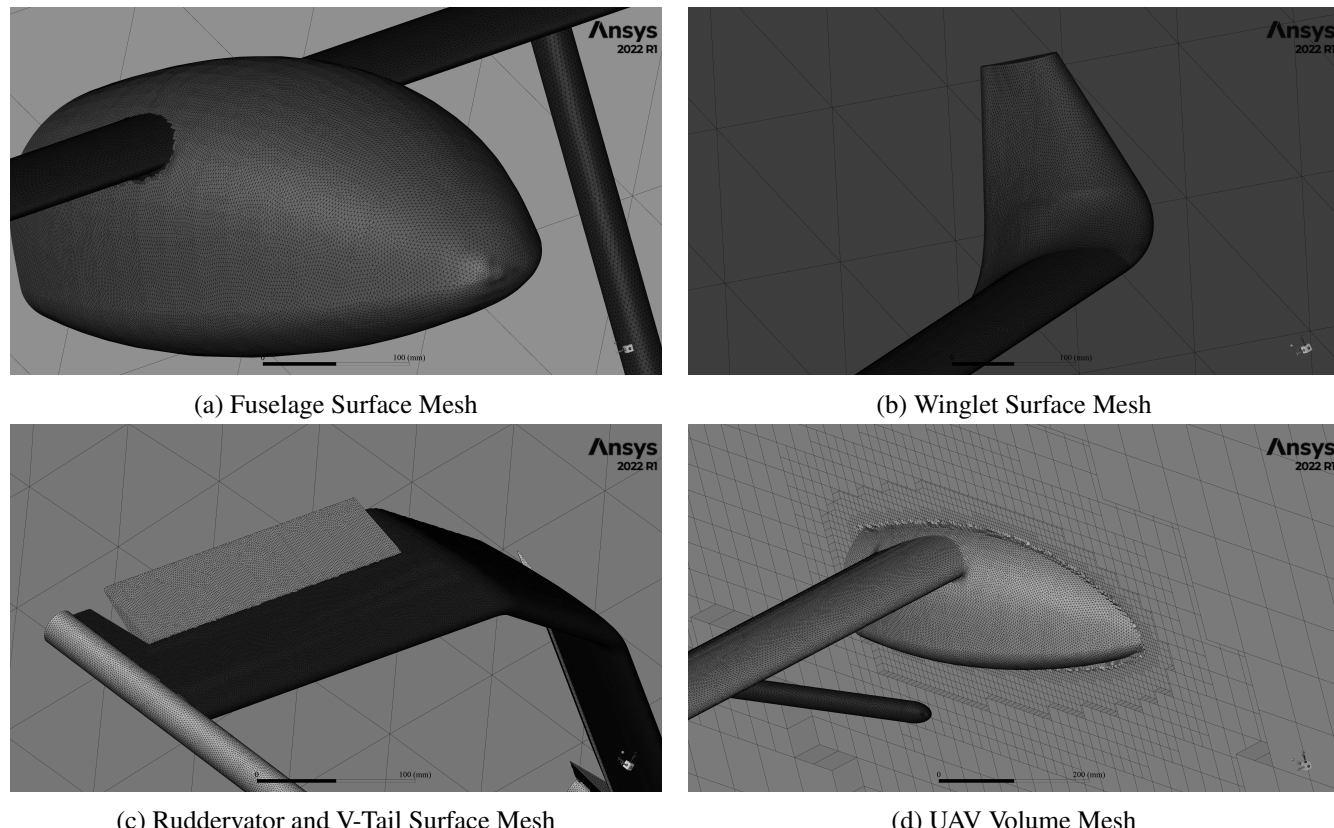


Figure D.4: Mesh Results Obtained after Mesh Independence Study

D.5 CFD Results

Reynolds-Averaged–Navier–Stokes (RANS) equations were solved along with $k - \omega - SST$ turbulence model. Cruise boundary conditions were used, since it is the longest phase of the UAV’s mission. The freestream velocity is set to 27m/s and the ambient conditions correspond to a flight altitude of 4000m . A wide range of angle of attacks are examined ranging from -4° to 26° .

D.5.1 Aircraft Performance

This section presents results for the wing performance as well as the overall UAV. Figure D.6 shows the C_L versus α curve for three cases: Analytical without winglet, wing CFD with winglet and wing CFD without winglet. From the table, it can be observed that the CFD results for the wing provide a lower lift coefficient compared to the analytical results, this is due to boundary layer effects and flow separation. However, when the winglets are added to the same wing, there is about 20 % increase in L/D ration of the wing, providing more lift by reducing lift-induced drag.

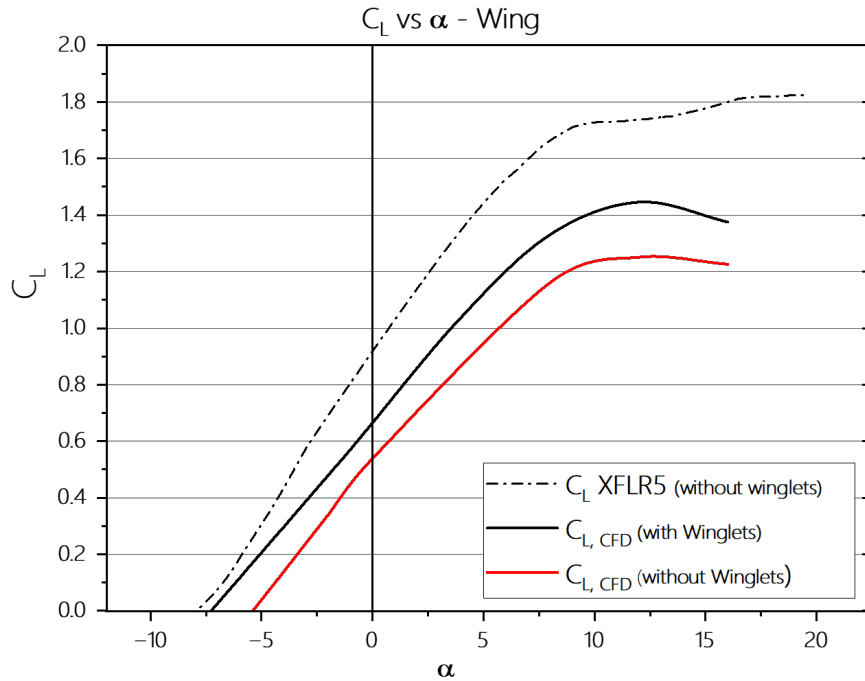


Figure D.5: Lift Coefficient vs. Angle of Attack - Wing Comparison.

Figure D.6 and Figure D.7 show the lift coefficient curve and the drag polar of the aircraft respectively. The aircraft lift coefficient curve is similar to the analytical curve calculated using XFLR5. The CFD curve shows the stall angle to be around 16° . At lower angle of attacks, where the boundary layer separation does not occur, the two curves are in agreement. However, as the angle of attack increases, the boundary layer separation comes into play and the analytical models cannot predict the stall. Figure D.7 shows the drag polar of the entire UAV - this includes the landing gears. CFD revealed that the landing gears have a drag penalty of about 5.5N . This is the reason for the drag polar to shift towards the right from the analytical curve (since landing gears were not modeled in the analytical model).

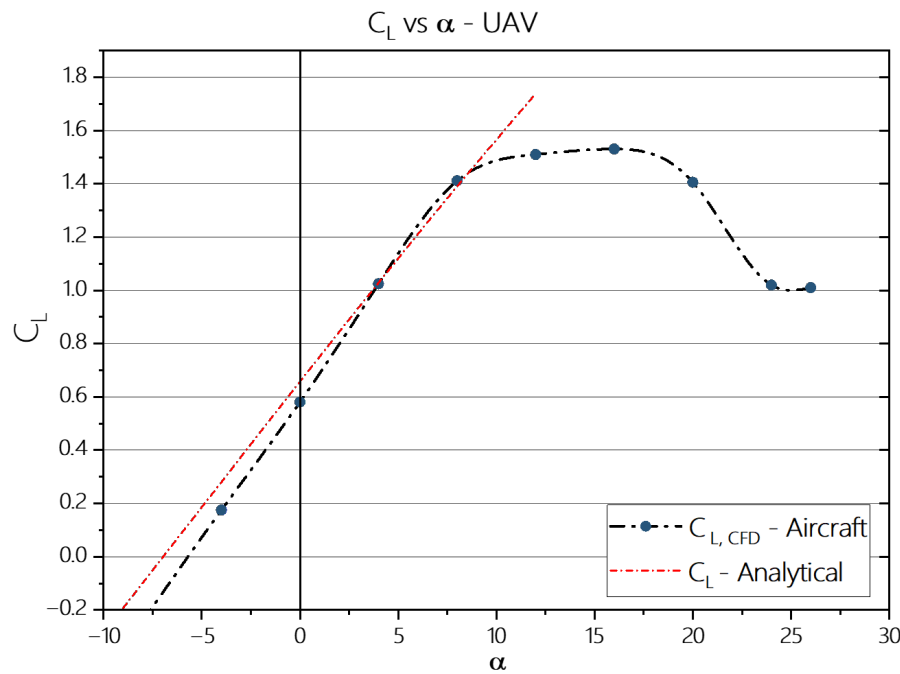


Figure D.6: Lift Coefficient vs. Angle of Attack - UAV.

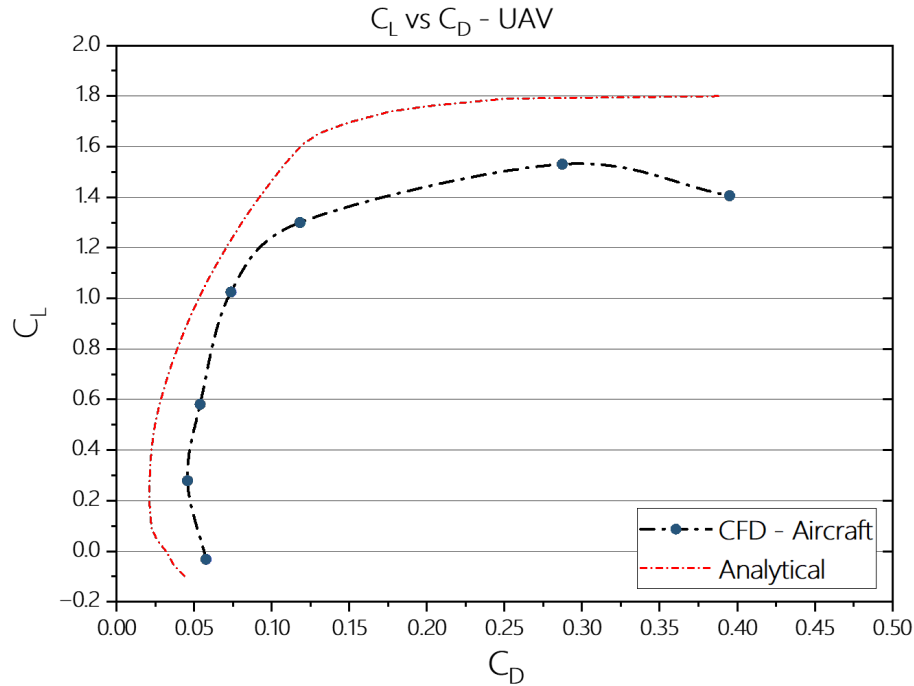


Figure D.7: Drag Polar - UAV.

D.5.2 Aircraft Roll

All the simulations seen above has been made with the same meshing process. Case 4 has a slightly different mesh because the ailerons needed to be analyzed separately from the rest of the aircraft to obtain the forces for the

Case Number	Case Description	Min cell size (mm)	Max Cell Size (mm)	Total Cells	Roll Moment (Nm)	Yaw Moment (Nm)	Pitch Moment (Nm)	Lift (N)	Drag (N)
1	4000 m; 27 m/s	0.9	200	4,866,940	-20.92	0.53	2.99	62.82	13.61
2	4000 m; 22 m/s	0.9	200	4,866,940	-13.84	0.36	1.93	41.31	9.15
3	Sea level; 27 m/s	0.9	200	4,866,940	-31.44	0.84	4.66	95.63	19.92
4	Sea level; 47.35 m/s	0.9	200	4,842,656	-97.22	3.51	-75.71	296.08	61.53

Table D.3: Results of the Simulations with the Ailerons at a 20-degree Inclination

hinge moment. In all cases, the left aileron is deflected down and the right aileron is deflected up. The angle of attack is 0 degree for all simulations seen here.

D.5.3 Aircraft Pitch and Yaw

With the ruddervator dimensions determined, the subsequent phase involved subjecting the design to numerous simulations using ANSYS. The simulations explored critical scenarios, including pitch-up, pitch-down, and yawing right, each executed at a maximum deflection of 20 degrees, while the ailerons maintained a neutral position.

Table D.4: CFD Results for Pitch and Yaw

Maneuver	Lift (N)	Drag (N)	Moment (Nm)	Force on Ruddervator (N)	Hinge Moment CFD (N-m)	Hinge Moment XFLR5 (N-m)
Pitch Up	101.39	19.00	25.10	1.84	0.085	0.016
Pitch Down	112.26	14.37	-9.76	1.16	0.054	0.011
Yaw Right	93.59	14.53	5.96	1.35	0.062	0.015

The CFD was done for conditions that represent air properties at 4000m, and at an angle of attack of 0 degrees. The results overview of the CFD simulations are summarized in Table D.4 above, the initial two columns present data on lift and drag acting on the entire drone assembly. Concurrently, the third column details the moments generated during pitch and yaw maneuvers around the y and z axes, respectively, encompassing the entire assembly. Then, the fourth column specifies the total force acting on a single ruddervator in the y-direction.

Transitioning to the following columns, we examine the outcomes derived from two methodologies—Computational Fluid Dynamics (CFD) and XFLR5—for computing the hinge moment of a singular ruddervator. The first approach entails using the force exerted on the ruddervator, presuming its application at a specific point along the trailing edge. This force is then multiplied by the distance to the quarter chord, yielding the resultant moment. It is crucial to acknowledge that this methodology tends to overestimate the actuator's size, rendering it less desirable. On the other hand, the second method involves utilizing the inherent hinge moment calculator within the XFLR5 software, promising a more precise evaluation. This alternative is expected to provide enhanced accuracy in determining the hinge moment, making it a preferable choice for our actuator choice considerations.

The sizing of the ruddervators will undergo validation through the deployment of XPLANE—a simulation software. This validation process aims to ensure that the aircraft can effectively meet the previously set requirement of achieving a pitch rate of 20 degrees per second. Also, XPLANE will be used to visualize all the moments generated by the ruddervators. This includes examining how a pitch-up movement introduces a slight yaw moment and vice versa.

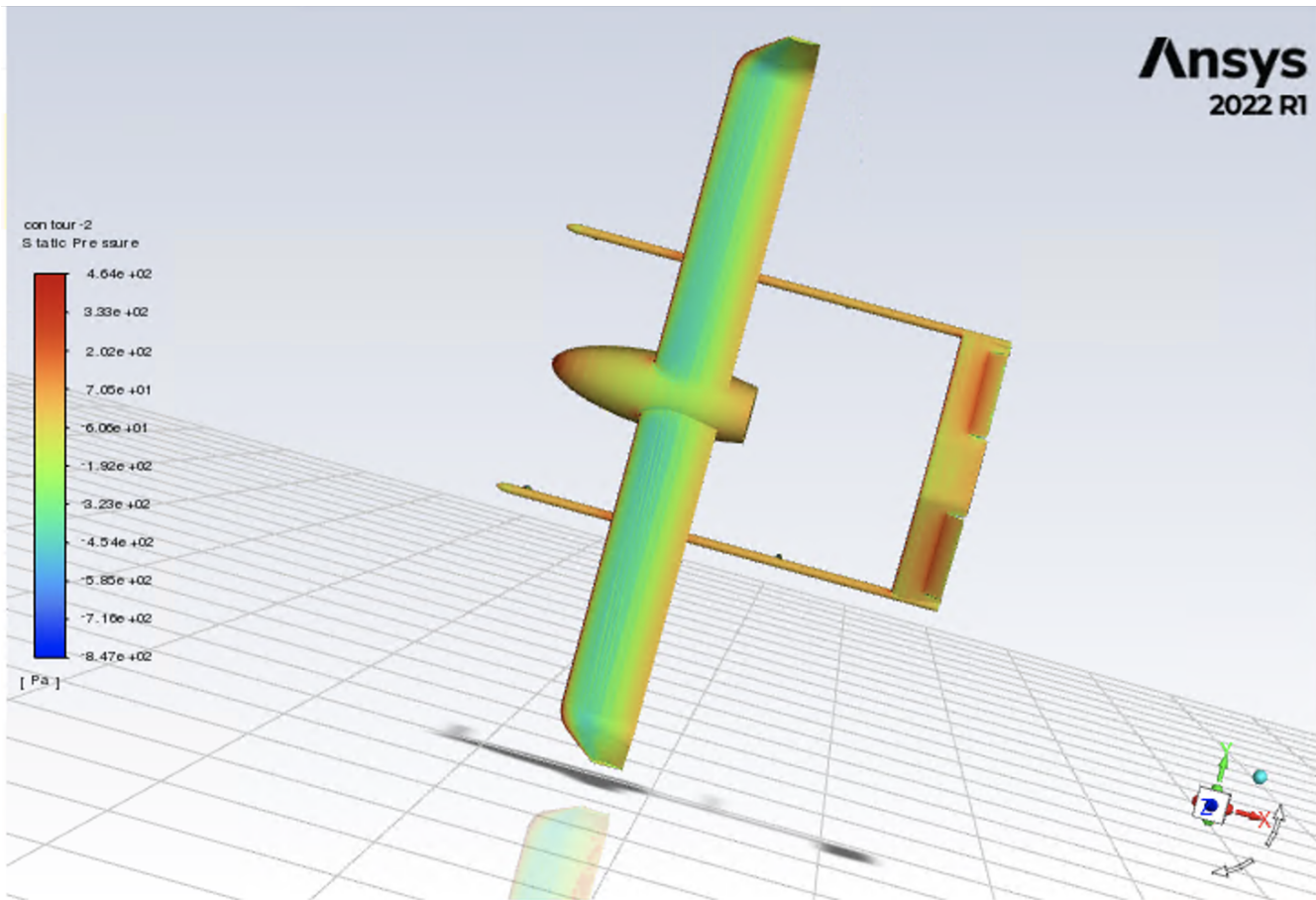


Figure D.8: Total Pressure Contours for Yaw right

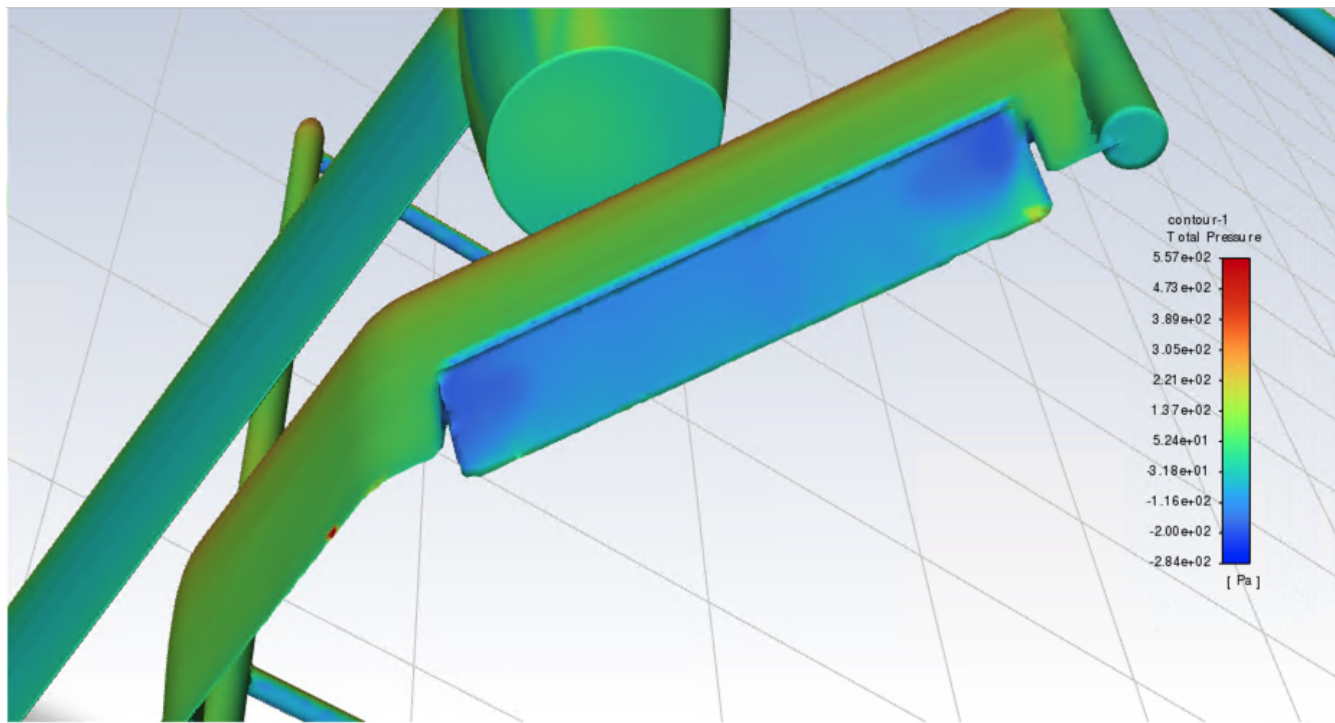


Figure D.9: Static Pressure Contours for Pitch Up

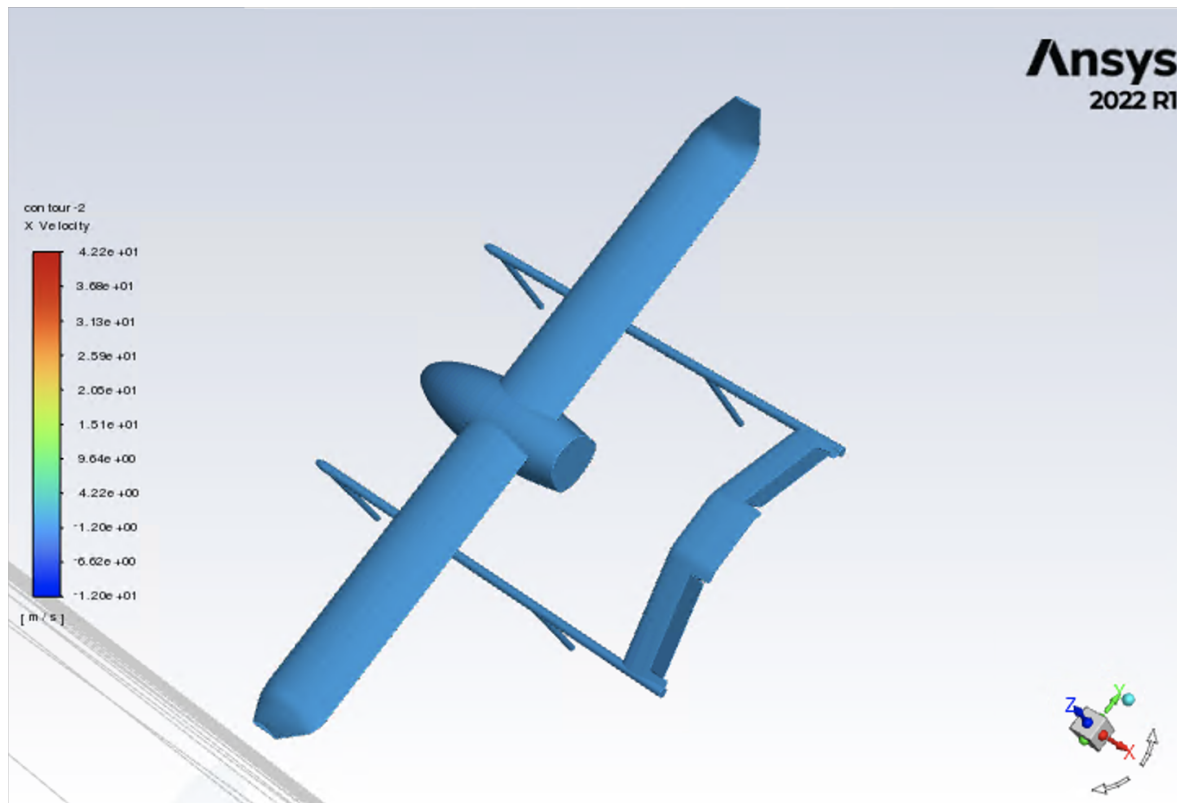


Figure D.10: Local Velocity Contours for Pitch Up

E Test Plan

REFERENCE STANDARD

The text in this test plan follows the format provided by 412TW-PA-21099 U.S AIRFOIRCE Technical Information Handbook titled “Test Plan Author’s Guide” [8]. Any formulation of section titles similar to the template provided by the aforementioned military standard is intentional for a clear depiction of the presented information. Distribution has been permitted by any authoring parties. Compliance with regional (Canadian) standards needs to be checked.

E.1 Introduction

The following test plan describes the scope, test objectives, test procedures, and result reporting methods for the “Aerodynamics team test plan”. The overall test objective is to validate requirements established from the aerodynamics team’s design deliverables. Validation and verification testing was requested by the AERO490 Capstone’s Integration Team to the capstone aerodynamics team. The organization “developing, operating and executing” the tests is the aerodynamics team, until further transmission of duties to the validation testing team, subsequently to the Integration team [8]. The stakeholders of the test plan are the AERO490 capstone program management team, the integration team, customers of the designed product as well as any future disciplines involved with manufacturing, purchasing, reviewing and/or presenting information contained in the test plan. The scheduled testing start date is January 2023 at Concordia University and will consist of about 10 hours of ground testing and 10 hours of flight testing, on behalf of the aerodynamics team alone.

E.1.1 Background

This test plan mainly describes two types of tests which will be carried out: flight testing and wind tunnel testing. Both tests will be carried out to validate and/or verify requirements established by the aerodynamics team to meet desired performance qualities of the product (the “Thunderbird Eco Surveillance drone”). Furthermore, testing is done to present accurate and actual performance characteristics of the aforementioned design product, the “Thunderbird Eco Surveillance” drone. Prior to testing, the design product underwent one conceptual, one preliminary, one detailed and one critical design phase over the months of September 2023-December 2023. Testing shall contribute to the drone’s design “freeze” prior and concurrent to manufacturing. Prior to testing, hand calculations and simulations through software have been carried out to establish design characteristics which shall be verified and/or validated through testing. Significant results from flight simulators and hand calculations include key aerodynamic and dimensional descriptors of the wing, tail, fuselage, control surfaces and other possible airframe surfaces. To approve the initiation of product testing, the following prerequisite must be met: the “Thunderbird Eco Surveillance” drone will have a printed DMU “digital mock-up” which has been finalized and approved by all design departments for at least three (3) weeks prior to testing, with no major changes occurring to the product prototype in the days preceding or during the execution of the tests. Failure to comply with the above requirements will lead to immediate rejection of test results and/or the conclusions emanating from the testing to become obsolete. This will require re-drafting of the test plan and to start over all tests to comply with the new design.

E.1.2 Test Item Description

The product which shall be tested is the fixed wing, V-TOL Unmanned Aerial Vehicle (UAV) titled “Thunderbird Eco Surveillance”. The tested structures shall be a prototype (3D printed, manufactured parts and/or samples) of the drone. The required configurations of the prototype are: overall model, separate wing and/or tail as required, tail with deflecting ruddervators, wing with deflecting ailerons, etc. The tested prototype will be a scaled down representation of the final product with its actual dimensions finalized so tested aerodynamic features will be representative of actual flights of the drone. Any deflections needed to be demonstrated by the control surfaces will be either achieved with appropriate equipment or physically simulated with said equipment (e.g. servos). The tested prototype may be affected by the wind tunnel and by flight conditions during testing. Mitigation measures shall be implemented to prevent the state of the prototype to be adversely affected by the tests. Requirements referred to or used to derive the following test procedures is available with the aerodynamics team.

E.2 Test Resource Requirements

The following section lists the resources and tools required to conduct the testing. Specific testing equipment as well as tools (software), ranges and laboratories will also be listed below.

E.2.1 Test Facilities, Ranges and Resources

Wind tunnel and flight testing shall be conducted at the Concordia University Hall building (tenth floor). Civil airspace, such as ranges, to conduct flight testing may also be used as required by the test requirements. Ranges will be specified as needed. Legal ranges and airspace for testing shall be dictated by Transport Canada and/or any other civil aviation authorities as required. Other legal rules and regulations pertaining to flight testing shall be provided by the Integration team.

E.2.2 Test System/Aircraft

The tested UAV shall be the designed V-TOL surveillance drone titled “Thunderbird Eco Surveillance”. Technical documentation pertaining to the design product can be found in the AERO490 Capstone database. Flight certification requirements, propulsion system operating limitations and other interdisciplinary constraints shall be provided by the Integration team, as needed.

E.2.3 Instrumentation and Parameter requirements

The equipment required for testing is a Boundary-Layer Wind Tunnel with the following specifications [1]:

- Type: Open-circuit, blowdown tunnel.
- Dimensions (L x W x H): 12 m x 1.8 m x 1.8 m.
- Maximum air speed (test section): 14.0 m/s out of a range of 4.7-14 m/s

E.2.4 Support Vehicles/Aircraft

A transport vehicle (van or truck) shall be selected to carry any tested parts of the designed prototype of the “Thunderbird Eco Surveillance” drone to tests sites, as needed.

E.2.5 Safety Considerations

Any safety plan for the testing phase shall be drafted based on safety recommendations suggested by the Integration team and aerospace standards, as needed. Safety consideration for safe wind tunnel usage and indoor flight testing shall be specified as needed.

E.2.6 Security requirements

The wind tunnel test shall be carried out in the presence of permitted laboratory technicians and/or staff as needed. Permission for indoors flight testing on school grounds shall be taken from the required school authorities. Indoor flight testing shall be carried out under the supervision of appointed employees, as needed. Other regulations concerning the provision of adequate protection in the planning of the tests, execution of the tests, test procedures, data replication or distribution and data analysis will be consulted from the Integration team as needed. Other personnel required for secure testing operations and communications shall be recommended by the Integration team.

E.2.7 Key stakeholders contact information

Table E.1 presents the list of delegates supervising and executing the tests lists the main personnel responsible for the execution of the test and the subsequent analysis and handling of test results. Note that the acronym PEM stands for Project Engineering Management. The name of the departments with updated names or that will become obsolete in future design stages has been followed with the ‘former’ descriptor. An index for the organization of the departments is provided in the document titled ‘Workpacks’, in the AERO490 Capstone’s database.

Table E.1: List of delegates supervising and executing the tests

Name	Role	Organization or department
TBD	Project lead of testing	Testing team
Matia Komsic	Program manager	PEM, WP4 (former)
Francisco Rivadeneira	Program manager	PEM, WP2 (former)
Bachar Khouri	Project engineer	PEM, WP1 (former)
Paramvir Lobana	Discipline Engineer	WP2 (former, lead)
TBD	Flight Test Engineer	Testing team
Cedric Chinn	Project Pilot	WP5 (former, lead)
TBD	External test lead	Optional Aviation Authority
Johnathan Liscouet, Dr.	Range manager (indoors and outdoors)	Concordia University, MIAE dept.

E.2.8 Test Environment Requirements

For indoors flight testing, the test environment shall have sufficient clearance (in terms of height, width, and length of the test range) for safe operation of the drone indoors and to prevent damages to prototype(s). Flight testing shall be carried out during specified schedules based on the required personnel's availabilities, as needed. This schedule will be drafted by the integration and engineering project management team. For outdoors testing, range location and specifications, time, dates, and appropriate weather conditions for safe operation shall be specified for safe operation of drone and to prevent damages to the prototype. Schedule for wind tunnel testing at the Concordia Aerospace Testing Lab (Hall Building, tenth floor) shall be provided by the laboratory staff based on the room's availabilities. No specific test environment requirements are considered unless specified by the Integration team, Concordia staff or the range staff.

E.2.9 Environmental Impact Assessment

Based on 32 CFR 989, Part 989 – *Environmental Impact Analysis Process (EIAP)* [X], an assessment of the environmental impact of indoors and outdoors flight testing, as well as wind tunnel testing, shall be conducted by the integration team. A checklist will be provided by the latter team, if needed. If no significant impacts on the human environment are identified, tests required by the aerodynamics department can be carried out as planned.

E.3 TEST AND EVALUATION

There will be 5 test stages, as defined in the V&V (verification and validation) diagram provided by the aerodynamics department and the integration team. Data will be documented and verified using hand calculations (surfaces sizing and thin airfoil theory) and the software specified in the section titled "Modeling and Simulation Resources". Documentation for result build up shall be carried out at the same location accessed through Github, in a Jupyter notebook dedicated for iterations of aerodynamics calculations. Results from computational analyses (e.g. Ansys) will also be kept with other results used to verify the data which will be validated through testing. Modeling and simulation methods and/or tools have been defined in previous sections.

E.3.1 General Test Objectives (GTOs) and Specific Test Objectives (STOs)

This section is outlined as in the 412TW-PA-21099 Handbook [8].

GTOs	STOs	MOPS
GTO 1 – Check that the design meets performance requirements for the specified mission profile.	<p>STO 1.1 Check that the airfoil meets the requirement of having a $C_l > 1.5$.</p> <p>STO 1.2 Check that the wing meets the requirement of providing over 92 N of Lift at cruise as stated in the requirements.</p>	<p>MOP 1.1.1 Lift coefficient, C_l</p> <p>MOP 1.1.2 Lift (force), in Newtons (N)</p>
GTO 2 – Check that the design meets maneuverability and stability requirements.	<p>STO 2.1 Check that the tail provides static longitudinal stability with a static margin of 5-15%.</p> <p>STO 2.2 Check that the tail contributes sufficient stability during 2 longitudinal and 3 lateral perturbation modes.</p> <p>STO 2.3 Check that the ailerons provide sufficient roll control.</p>	<p>N/A</p> <p>MOP 2.1.2 See section 2.4.2.2</p> <p>MOP 2.1.3 Rolling moment, in Newton-meters (N-m)</p>
	<p>STO 2.4 Check that the ailerons meet the requirement of achieving a roll rate of 30° in 1.3 s with a maximum deflection of $\delta = 25^\circ$.</p> <p>STO 2.5 Check that the ruddervator meet the requirement of achieving a pitch rate of 20°/s at a full deflection of $\delta = 30^\circ$.</p>	<p>MOP 2.1.4 Roll rate, in degrees per second ($^\circ/\text{s}$)</p> <p>MOP 2.1.5 Pitching rate, degrees per second ($^\circ/\text{s}$)</p>

Table E.2: General Test Objectives (GTOs) and Specific Test objectives (STOs)

E.3.2 Potential Impacts of Completion Criteria

This section describes factors that could prevent meeting the desired test objectives. Events affecting testing and subsequent test results will also be listed. Risks during testing shall also be elaborated in this section:

No potential risks of carrying out either wind tunnel test(s) or flight test(s) have been outlined by the Integration team. This section is subject to changes.

The desired test objectives from either the wind tunnel test(s) or the flight test(s) will not be achieved if the tested prototype does not behave systematically or physically as desired. Prototype failures that may affect test performance include, but are not limited to, failing control surfaces, inadequate printing of airframe surfaces, damaged prototype components or structures, inadequate center of gravity location upon printing, etc.

E.4 GTO 1 – Validation testing of designed drone’s aerodynamic performance

E.4.1 STO 1.1– Validation testing of lift coefficient of the airfoil

MOP 1.1.1 – Lift coefficient The lift coefficient (c_l) is proportional to the lift force generated by an object, thus contributing to the determination of its lift. Lift is the force countering gravity, thus allowing any aerial vehicle to remain airborne. For the purpose of validation, it shall be measured at the airfoil section to validate that the requirement specified in Table 2: General Test Objectives (GTOs) and Specific Test objectives (STOs) has been met.

Test Methodology Measurement of the airfoil lift coefficient shall be carried out through wind tunnel testing. The specifications of the wind tunnel which shall be used is given in the section titled “Instrumentation and Parameter Requirements”. Inputs to the testing apparatus includes the airflow velocity, which shall be set to $V = 27 \text{ m/s}$ to match cruise conditions. Testing shall be done using a 3D printed section of the wing which shall be scaled down to about 22% of its actual size. The wing section shall be mounted at an angle of attack of zero degrees ($\text{AOA} = 0^\circ$). The wind tunnel shall be run five times for redundancy and accuracy of the results.

Test Completion Criteria Following the calibration of the equipment and the mounting of the wing section, the wind tunnel shall be run until the lift coefficient reaches its maximum value, with a fluctuation allowance of ± 0.01 max. of the lift coefficient per 5-10 seconds of wait.

Expected Test Results Based on previous stability analysis on XFOIL and computational fluid dynamics (CFD) on Ansys, the airfoil lift coefficient is expected to be $c_l = 1.9$. The expected lift coefficient can also be taken from previous hand calculations, but for more accuracy, the updated value from simulations will be considered. This measure of performance (MOP) is expected to be deficient, but testing is planned to ensure that the wing lift is sufficient for the given mission profile. A targeted airfoil lift coefficient of 1.5 is needed for the design product to attain its intended endurance performance.

Data requirements Refer to this test’s methodology for the required wind tunnel input and wing mount configurations.

Data analysis and Final Data Products The results for this test shall be the lift coefficients of the airfoil. They will be tabulated per number of trials. The average of all five trials shall be used to establish conclusions on performance requirements. For data validation purposes, the exact angle at which the wing section is mounted from the digital readout will be taken. This is to assess the reliability and accuracy of the results. Any other environmental conditions relevant to the data analysis (e.g., room temperature, air quality, or any other relevant environmental data) will be recorded, as needed.

Evaluation Criteria Due to the criticality of achieving a lift coefficient of $c_l = 1.5$ for sufficient endurance of the designed drone, any results over $c_l = 1.5$ will be considered to be good. Results are only considered sufficient/acceptable if nearly equal to 1.5 ± 0.01 . Results are to be rejected if the average c_l value is significantly lower than 1.5.

E.4.2 STO 1.2 – Validation testing of the lift from the wing

MOP 1.1.2 – Lift force Lift is the force countering gravity, thus allowing any aerial vehicle to remain airborne. For the purpose of validation, it shall be measured at the airfoil section. The lift shall be measured for the entire wing to validate that the requirement from Table 2 will be met by the designed product.

Test Methodology The same methodology as outlined in the previous test methodology shall be employed for this test. One distinction of this test is the measured value (i.e., results of the tests), which shall be the lift force directly in this case. The tested model shall be a scaled down 3D print of the entire wing and its dimensions. Furthermore, the wing model mounted in the wind tunnel shall be the entire wing with (its actual dimensions) scaled down to 22%.

Test Completion Criteria Following the calibration of the equipment and the mounting of the wing section, the wind tunnel shall be run until the lift value reaches its maximum value, with a fluctuation allowance of ± 2.00 max. of the lift per 10-30 seconds of waiting.

Expected Test Results Based on the latest computational fluid dynamics (CFD) on Ansys, the overall lift of the UAV is expected to be 110 N. This measure of performance (MOP) is expected to be unacceptable, but testing is planned to ensure that the wing lift is sufficient for the given mission profile. A targeted airfoil lift coefficient of 1.5 is needed for the designed drone to attain its intended endurance performance.

Data requirements Refer to the previous test methodology for the required wind tunnel input and wing mount configurations.

Data analysis and Final Data Products The results for this test shall be the lift force measured by strain gauges on the wing model. They will be tabulated per number of trials. The average of all five trials shall be used to establish conclusions on performance requirements. For data validation purposes, the exact angle at which the wing section is mounted from the digital readout will be taken. This is to assess the reliability and accuracy of the results. Any other environmental conditions relevant to the data analysis (e.g., room temperature, air quality, or any other relevant environmental data) will be recorded, as needed.

Expected Test Results

- The results are considered to be good if: Lift ≤ 110 N
- The results are considered to be acceptable if: $92 \text{ N} \leq \text{Lift} \leq 100 \text{ N}$
- The results are to be rejected if: Lift is lower than 92 N.

E.5 GTO 2 – Validation testing of designed drone's maneuverability and stability

E.5.1 STO 2.1 – Validation testing of tail static stability

MOP 2.1.1 – Section Not Applied The result of this test shall be visual observations of the design drone's behaviour in flight. Therefore, there are no attributable measures of performance (MoP).

Test Methodology The test of this section shall be a flight test of a scaled model of the final design, or the final assembled drone itself. The “Thunderbird Eco Surveillance” drone model shall be submitted to a disturbance in flight by increasing its angle of attack in flight. The trimming of the aircraft shall be visually confirmed at different flight AOAs. For the safety of the final product, the drone shall be flown at an altitude of no more than 10 meters during disturbances. The drone shall first be flown to an altitude of 10 meters above ground level (AGL). Following 3-5 minutes of steady, level flight, the drone’s angle of attack shall be suddenly increased by increments of 5 degrees, starting from zero degrees. The flight test shall be repeated for a total of 1 flight session, during which 3 disturbances will be caused (at $\text{AOA} = 5^\circ, 10^\circ, 15^\circ$) to simulate a nose-up pitching moment of the drone. Each angle of attack shall be imposed on the drone 3 times each.

Test Completion Criteria Each trial (for different values of the angle of attack) shall be ended if trimming is not achieved within 5-10 seconds following the pitch up motion of the drone. The test shall be concluded once all trials have been completed, for all angles of attack.

Expected Test Results Based on stability analysis carried out through software (XFLOW and XFLR5), it is expected than the drone will trim back to straight and level flight following induced pitch up moments of the drone.

Data requirements The data inputs shall be a flight controller (or a program which can execute the same tasks) in which the angle of attack shall be the input. This input must lead to a change in the actual flight angle of attack of the drone. The test points shall be $5^\circ, 10^\circ, 15^\circ$.

Data analysis and Final Data Products The results from this test shall be visual observations of the drone’s reaction to certain pitch-up inputs. These observations shall be documented during testing.

Expected Test Results The test shall be considered successful and conclusive if: drone trimming reaction is observed upon inducing a nose-up pitch.

The test shall be considered borderline if: angle of attack inputs do not lead to the drone failing or stalling during testing, but the drone does not trim back to stable flight.

The test shall be considered as failed if: the drone stalls and/or fails when inducing a nose-up pitching moment.

E.5.2 STO 2.2– Validation testing of tail stability during maneuvers

MOP 2.1.2 – Various For this test, the following disturbance manoeuvres shall be defined: Disturbance manoeuvres in longitudinal stability: short period phugoid, long period phugoid. Disturbance manoeuvres in lateral stability: Roll, Dutch Roll and Spiral. Visual depictions for all of the above manoeuvres are provided in Appendix 6.2. Measures of performance specific to each disturbance manoeuvres are:

- Period and damping ratio for phugoid oscillations.
- Natural frequency and damping ratio of short period oscillations during controlled pitch inputs.
- Frequency and damping ratio of Dutch roll oscillations induced by lateral disturbances.
- Measure of the roll rate and time to reach steady-state roll rate during controlled aileron input tests.
- Measure of the roll and sideslip angles during controlled sideslip tests.

Test Methodology For this test, disturbances shall be simulated on the control surfaces' Pixhawk program. Simulated disturbances are as listed in the previous section:

- Phugoid Oscillations.
- Short period oscillations with controlled pitch.
- Dutch roll oscillations.
- Aileron input tests.
- Sideslip tests.

This test has been delegated to the AERO490 Capstone Command & Control team as hardware programming related to control surfaces has been assigned to the avionics department. Readers should send inquiries to the C&C team for further details on inputs.

Test Completion Criteria This test has been delegated to the AERO490 Capstone Command & Control team as hardware programming related to control surfaces has been assigned to the avionics department. Readers should send inquiries to the C&C team for further details on test completion criteria.

Expected Test Results This test has been delegated to the AERO490 Capstone Command & Control team as hardware programming related to control surfaces has been assigned to the avionics department. No expected result has been proposed by the Command & Control department.

Data requirements This test has been delegated to the AERO490 Capstone Command & Control team as hardware programming related to control surfaces has been assigned to the avionics department. Readers should send inquiries to the C&C team for further details on inputs.

Data analysis and Final Data Products See this test's MOP section for details on data products resulting from this test.

Expected Test Results This test has been delegated to the AERO490 Capstone Command & Control team as hardware programming related to control surfaces has been assigned to the avionics department. No evaluation criteria have been proposed by the Command & Control department.

E.5.3 STO 2.3– Validation testing of tail rolling moment during maneuvers

MOP 2.1.3 – Rolling moment Ailerons are the main or primary control systems found on aircrafts. They allow a motion known as the “rolling” the aircraft. Rolling the aircraft refers to rotating or tilting the aircraft about the longitudinal axis. The rolling moment is an indication of actuation loads required for the ailerons to perform as desired for maneuverability.

Test Methodology The actuation of the ailerons for the design product shall be simulated physically using a test rig or during flight testing. In both cases, the test rig shall consist of a scaled printed model of the drone. The control surfaces of this model (or final product) should perform at the maximum ability intended from the control surfaces for test results to be valid. Following assembly of the aileron surface and actuator on an acceptable rig, the aileron deflection shall be automated using electrical data transmission, whereby the inputs shall be entered in a software of choice (e.g. flight controller). The output should be such, that the rolling moment can be read directly from the actuator, by mounting load cells (or other force sensors) directly on the surfaces or actuators [3]. This test rig shall fully show the synchronized deflection of all aileron surfaces on either side of the wing to yield acceptable results. This experiment shall be repeated 5 times with a stationary rig for redundancy and accuracy. For flight

testing, roll control shall be observed during actuation of the ailerons at loiter and approach altitudes and velocities. Flight testing should only be conducted once.

Test Completion Criteria Following the assembly of the aileron surface rig on both sides of the wing, the aileron deflection shall be simulated such that the maximum deflection expected of $\delta = 25^\circ$ is reached. When maximum deflection is reached, the test will be concluded.

Expected Test Results Following simulations of aileron deflection on Ansys and hand calculations, Table E.3 summarizes the expected results for the rolling moment at different flight conditions.

Table E.3: Rolling moment expected results for different flight conditions.

Conditions	Analytical results (Nm)	CFD Results (Nm)
4000 m, 27 m/s	21.98	20.92
4000 m, 22 m/s	14.59	13.84
0 m, 27 m/s	32.86	31.44

Data requirements Data requirements for this test shall be an aileron deflection program for the design prototype, whereby its inputs will translate into the actual aileron's motion (e.g. flight controller). Furthermore, inputs must be defined for the program itself, i.e., desired angle of deflection of the ailerons. These deflection angles will start from zero and increase by increments of 5° for the recorded datapoints.

Data analysis and Final Data Products The results for this test shall be the loads on the aileron surface for various deflection angles as defined in the previous section. Said loads shall be used to calculate the actual rolling moment achieved from the ailerons.

Expected Test Results

- The results are considered to be good if: $31.44 \text{ N-m} \leq \text{The rolling moment} \leq 32.86 \text{ N-m}$
- The results are considered to be acceptable if: $20.92 \text{ N-m} \leq \text{Rolling moment} \leq 21.98 \text{ N-m}$
- The results are considered to be “borderline” if [1]: $13.84 \text{ N-m} \leq \text{Rolling moment} \leq 14.59 \text{ N-m}$
- Any results which are not contained in the above ranges are to be rejected.

E.5.4 STO 2.4 – Validation testing of aileron roll rate for maneuverability.

MOP 2.1.4 – Rolling rate See the introduction of the previous test. The roll rate is the change in roll angle achieved per units of time, or seconds.

Test Methodology See section the previous test description for the test rig description. For this test, a fully scaled model of the designed drone shall be flown, whereby the desired roll rate can be programmed from piloting controls. The time required for the desired roll angle inputs to be fully reached shall be measured using a timer, or by other appropriate means of measuring the time to reach the roll angle. The time taken for the desired roll angle to be reached shall be measured during three (3) trials (for stationary test rig) for redundancy and accuracy. Said timer will be started at the beginning of the rolling motion of the drone and shall end following the achievement of the desired roll angle. This test shall be repeated 1-2 times maximum (for flight testing) for redundancy and accuracy. Control surfaces deflection angles or drone angular motion can be measured using variable resistors mounted on the control surfaces and wings [2].

Test Completion Criteria Following the assembly of the aileron surface rig on both sides of the wing, the drone shall be flown until a roll angle of 30° is reached.

Expected Test Results Based on hand calculations and validation using CFD analysis on Ansys, the expected time for the ailerons to lead the drone to a roll angle of 30° is approximately 1.3 seconds. In other terms, these results translated into an expected roll rate of $23.08^\circ/s$

Data requirements Data requirements for this test shall be a simulation or program allowing the pilot(s) to enter the desired roll angle of the drone. Other data requirements shall be the different roll angles tested, starting from zero to an increase in increments of 5-10 degrees until the roll angle value of 30° is reached.

Data analysis and Final Data Products The results from this test shall be the time required to achieve the roll angles specified in the above section. Furthermore, for verification of the validity and accuracy of the test, the aileron deflection angle during testing shall also be recorded.

Expected Test Results

- The results are considered to be good if: A roll angle of 30° is achieved in less than 1.3 s
- The results are considered to be acceptable if: A roll angle of 30° is achieved in 1.3s
- The results are to be rejected if: A roll angle of 30° is achieved in more than 1.3s.

E.5.5 STO 2.5– Validation testing of ruddervator pitch rate

MOP 2.1.5 – pitch rate Ruddervators are control surfaces used for aircrafts with V-tail configurations [4]. These control surfaces combine rudders and elevators and are actuated by the same pilot controls [4]. When actuated symmetrically, the ruddervators carry out the function of elevators to “pitch” the aircraft [4]. Pitching is the rotation of the aircraft about the lateral axis or defined by “nose up” and “nose down” reactions of an aircraft. The pitch rate is the change in the angle of pitch of an aircraft with respect to a unit of time, or seconds.

Test Methodology See the previous test description for details on the test rig intended for this test and the description of the test carried out for this section. The the time to achieve a certain pitch angle will be recorded, for pitch angle values starting from zero, and increasing to 20° by increments of 5 degrees. In this test, the deflection shall be of the ruddervators, and throughout the flight test, the ruddervator deflection angle shall be its maximum value of $\delta = 30^\circ$. This test shall be repeated 1-2 times maximum for redundancy and accuracy. Note that all ruddervator surfaces should be actuated to their expected actual capacity during the testing for test results to be valid. Control surfaces deflection angles or drone angular motion can be measured using variable resistors mounted on control surfaces and wings [2].

Test Completion Criteria Following the assembly of the ruddervator surfaces rig on both sides of the tail, the test shall be carried out until maximum ruddervator deflection angle of 30° has been reached while pitching the aircraft.

Expected Test Results Based on hand calculations and validation using CFD analyses on Ansys, the expected pitch rate should be $20^\circ/s$, or a time of almost 1 second required to pitch the design drone by 20° .

Data requirements Data requirements for this test shall be a ruddervator deflection program for the design prototype, whereby its inputs will translate into ruddervator motion and aircraft pitch. Furthermore, inputs must be defined for the program itself, i.e., the desired angles of deflection of the ruddervators and the desired pitch angles of the drone, which are described in section in the previous section.

Data analysis and Final Data Products The results of this test shall be the time required to achieve different pitch angles. Then, for the analysis of the validity and accuracy of this test, the actual ruddervator deflection shall also be recorded.

Expected Test Results

- The results are considered to be good if: the pitch rate $> 20^\circ/s$.
- The results are considered to be acceptable if: the pitch rate $= 20^\circ/s$.
- The results are to be rejected if: pitch rate $< 20^\circ/s$.

E.6 TEST CONDUCT

The AERO490 Capstone of Fall 2023 Testing Team will conduct the tests outlined in the section titled “TEST AND EVALUATION” of this report.

E.6.1 Readiness reviews

Test readiness review (TRR) shall be carried out concurrently with the testing or 1-2 days prior to final testing unless otherwise specified by the Integration team.

The attendees required to attend all testing phases and sessions are the testing team members outlined in Table 1. In the event of urgent testing being required, or for requesting permissions on site, the managers specified in Table 1 may be requested to attend test(s). For the flight testing, the pilot(s) listed in Table 1 are obligated to attend all flight-testing sessions. In cases of scheduling conflicts, pilot qualification and/or license level data may be requested from the Integration team for substituting the staff. Other mandatory attendees include any laboratory technician(s) if usage of any equipment by the testing team representatives is not allowed by said technicians.

Readiness to test is considered when the tested prototypes and/or models have been confirmed to be functional and/or appropriate by the authorizing staff. Readiness consideration will be given by the leads of testing outlined in E.1. If required, the program manager(s) and Integration team may approve the readiness to test of design models and/or parts. The objective of the testing phase is to make sure that the aerodynamic performance requirements, and all aerodynamic consideration(s) relevant to the overall drone performance, are met. Test results must be acceptable and safe to serve for design validation purposes. Areas of technical risk include lack of experience manipulating test requirements and/or in analyzing test results. Proximity to obstacles, such as human environment, during flight testing is another safety risk. Lastly, dysfunctional, or outdated test prototypes may pose a risk to validating results. An in-depth risk assessment of the test plan will be carried out by the Integration team, as required.

The design prototype status, such as its readiness for flight or testing, is information available to receive from the Integration team and program managers upon request. Test completion criteria may be reviewed based on changes in performance requirements to assess the adequacy of former results. The test procedures shall also be periodically reviewed upon critical design changes to assess the reliability of former results. Test schedules will be drafted and available with the Integration team and/or program manager and testing leads.

The wind tunnel (located at Hall building, 10th floor) is available for use upon request based on a set of availabilities for borrowing the equipment. Software for the analysis of results is always available from the Concordia University computers. Test documentation and results will be available with the aerodynamics team and the integration team. Test documentation must be updated monthly to reflect major or urgent design changes. Staff to ensure secure and safe execution of all tests conducted on Concordia School grounds and laboratories are available on demand during test sessions if requested. These are the laboratory technician and Concordia security personnel. Testing team member training include:

1. Mandatory reminder of rules for safe and ethical practices during testing if it is requested from program managers and laboratory technicians.

2. Mandatory quick training in how to use the testing apparatus (e.g. wind tunnel) for personnel safety and proper use of school property.
3. No in-depth technical training or qualification in laboratory sciences is required by any testing members unless requested by team member or program managers.
4. No in-depth technical training or qualification in laboratory sciences is required by any testing members unless requested by team member or program managers.

The applicable airworthiness standards and processes to aerodynamic testing shall be documented and provided by the Integration Team exclusively. All required detail on airworthiness should be requested by the responsible department(s).

For the execution of the tests, the following are the no-go criteria:

1. Tests cannot be conducted if major modifications have been made to the drone model depicted on the latest 3D print within the last 30 days as prefaced in the test plan.
2. Tests cannot be conducted on samples which do not reflect the most updated revision(s) of test plans drafted by any design department, including the aerodynamics department.
3. Tests cannot be conducted on testing samples which do not meet the minimum requirements for being valid for testing as specified in each individual tests listed the "Test and "Evaluation" section.

The tests have the go-ahead to be executed if:

1. Test plan has been approved by the authorities listed in Table 1 and at least one (1) expert in the field.
2. Test plan execution on Concordia school grounds has been approved and scheduled by laboratory technicians and security staff.
3. Test plan execution has been approved by program managers and implemented or acknowledged by the integration team.
4. Test plan is coherent with the test plan of other disciplines and is deemed feasible, financially efficient, time efficient and relevant by authorities and experts listed in Table 1 , including other disciplines.

Test data collection cards with brief testing procedures shall be provided to the testing crew upon request from the aerodynamics team. All test cards will be available electronically in a resources folder for the execution and data collection during testing. Prior to testing, a briefing and debriefing of 30-60 minutes should be expected and accounted for all individual tests scheduled. The content will be provided by the staff overseeing each test within 2 days before testing in a case-by-case manner and only if needed.

The status of the data analysis tools provided by Concordia, i.e., software on campus and off-campus (e.g. Ansys, Simulink, Concordia, X-Plane) is handled and distributed by the Concordia IT department and/or service desk(s). Readers are encouraged to find the requested information on the Concordia Website for technical assistance.

The reporting plan for the testing will be provided in section 4 and when requested following testing.

E.6.2 Pretest Briefing(s)

Pretest briefings will be sent to personnel (test team) executing the tests by the supervisors overseeing the testing. These briefings will be sent by email within the 2 days prior to any test. Instrumentation (e.g. wind tunnel) status and usage schedule can be requested from laboratory technician by email. Range status and availabilities for flight testing can be provided by the municipal authorities of the range location. The required testing software and hardware configuration is specified, if needed, in the "Testing and Evaluation" section. The test objectives and procedures, test completion and go/no-go criteria is provided in the "Testing and evaluation" section, along with the date requirements, unless otherwise specified on site. Refer to the latest test plan revisions for more details.

E.6.3 Test execution

The instrumentation usage and calibration procedures, laboratory rules and the layout of the test rooms can be requested from the laboratory personnel prior to testing. Testing team members and requested guests from other disciplines should assign roles and distribute tasks for the quick and efficient execution of the tests. For a proper organization and the safe execution of tests, tests shall be scheduled such that different types of tests will not be executed at the same time at the same location. No more than 6 member(s) will participate in a single test so as to not overcrowd the testing.

E.6.4 Post-test Briefing

All AERO490 Capstone members present during the testing, excluding non-testing team members (unless requested for input) and Concordia full-time personnel (e.g. laboratory supervisors or technicians) must attend post-test briefings. The chosen representative of the testing team lead is responsible for executing or assigning any present Capstone students with this task during all test sessions assigned to them. This post-test brief will address the following topics:

1. Any instrumentation issues which came up during the test to address them to the laboratory technicians, if any.
2. Verification that the post-test maintenance procedures for closing and returning equipment have been followed.
3. A summary of tests executed, which need to be reattempted, and which can be marked as completed.
4. Quick verification of tests results and their validity for future processes.
5. Quick briefing of the next design steps based on results (e.g. if tests need to be rescheduled, if re-design needs to be discussed, etc.)

E.6.5 Post-test Data Procedures

Following testing, any data collected which are deemed valid for further analysis and future design phases shall be kept in data cards by the aerodynamics team in a private folder for proper sorting. This data shall be available to other disciplines and external parties without requesting, if needed, when official test reports containing test results and interpretation are published. Prior to publishing, the test cards must be signed by the aerodynamics team lead and testing team lead pending the approval of program managers.

If data needs to be requested before the publishing of the test reports, requesting parties need to send their requests to the aerodynamics team lead, or testing team lead, using proper communication protocols. The leads may send data to requesting parties if the request is justified, or if the program managers allow the transmission of test results. Note that any request for data should be passed to the integration team first. External parties must always request data, in report form or data form, from integration first at any point in time.

E.7 Test Reporting

E.7.1 4.1 Data deficiency reporting

If any party from any discipline has any concern with the validation of test results, or if they deem the results to be problematic or unsafe for design purposes, they may address their concerns to the aerodynamics and/or testing team lead directly. This communication may only be done through a formal report or a memorandum with either of the following parties attached:

- Either program manager(s)
- Authorized expert or external contractor(s)

- Integration, or alternative team's lead or any other authorized delegate.

Senders need approval from their disciplinary team lead to address the issues and should give enough details about their concerns for further communication to be possible on the topic. Any informal methods of relaying this information (e.g. messaging via Teams, unauthorized emails) will be ignored. No decision will be made without having a meeting with involved parties first.

E.7.2 Quick look reports

The testing team in conjunction with the aerodynamics team will always prepare a “quick look report” [8] which will be sent to any relevant disciplines, requesting parties and managers. This report will contain the test sample tested (e.g. what model was used), the tested datapoints, the invalid datapoints, and a summary of the conclusions drawn on site following testing. This report shall be sent in the form of a memo within 24 hours of testing.

E.7.3 Preliminary Report of Results

If a technical report is requested sooner than a formal report may be drafted, a preliminary report of results may be provided for official presentation. Preliminary reports are also for test results which are not deemed conclusive, or for placeholder data. The preliminary report does not need to be as detailed as a full TR (technical report) and may be drafted to emphasize important data according to the aerodynamic team lead’s judgment.

E.7.4 Capability report

A capability report detailing all hand calculations and software analyses used to confirm, validate, or verify the test results may be drafted upon request from management [8]. This will serve as a reference to provide rationale(s) for testing or test conclusions made at a later stage and must be clear enough to understand the previous design steps easily. Alternatively, any of the previous design milestones report may be referred to as CRs. When that is the case, the team leads may direct any requesters to the proper file path if they desire.

E.7.5 Technical Information Memorandum/Handbook

After the finalization of the design of the ‘Thunderbird Surveillance’ drone, a “Technical Information Report” may be drafted to lists all tests executed with procedures and key conclusions [8]. This handbook will serve for future references and to easily repeat testing if necessary.

E.7.6 Technical Report (TR)

Following testing, a test report will be drafted to indicate all test results and consecutive recommendations [8]. Qualification status of the designed drone will also be updated pending the analysis of results [8]. Both steps will be documented in the TR [8].

E.7.7 Data packages (DP)

All data collected will be compiled in a data package for redistribution following the finalization of all testing phases and tests [8]. Refer to the appropriate section for procedures on requesting data prior to this timeline.

E.7.8 Test completion letter (TCL)

Following a test consisting only of data collection, a notice may be sent to stakeholders to notify them that a test has been completed [8]. This letter will not contain any analysis of results of subsequent recommendations and conclusions [8]. This letter may however warn of urgent results or warnings about the execution of the test (such as

failures, etc.). This is the recommended practice for notifying about the execution of a test which the aerodynamics team will look into using.

E.8 List of Acronyms and Abbreviations for Test Plan

- DMU – Digital mockup
- V-TOL – Vertical takeoff and Landing
- UAV – Unmanned Aerial Vehicle
- PEM – Engineering Project Management
- V&V – Verification and validation
- AOA – Angle of attack
- CFD – Computational Fluid Dynamics
- C&C – Command and control
- TRR – Test readiness review
- TR – Technical Report
- CR – Capability report
- DP – Data packages
- TCL – Test Completion Letter

E.9 Nomenclature for Test Plan

- C_l = Lift coefficient
- N = Newton
- m = Meters
- s = Seconds
- δ = Control surface deflection

E.10 Disturbance maneuvers

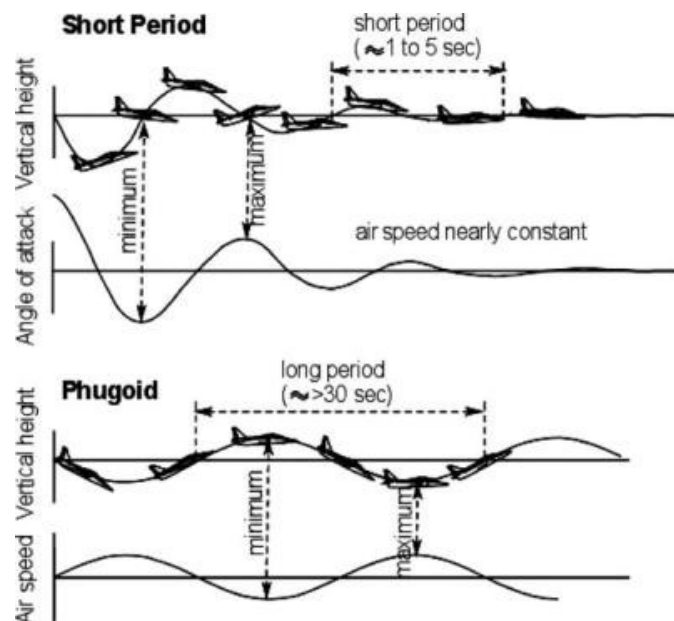


Figure E.1: Schematic of Phugoid and Short-Period Oscillation [10]

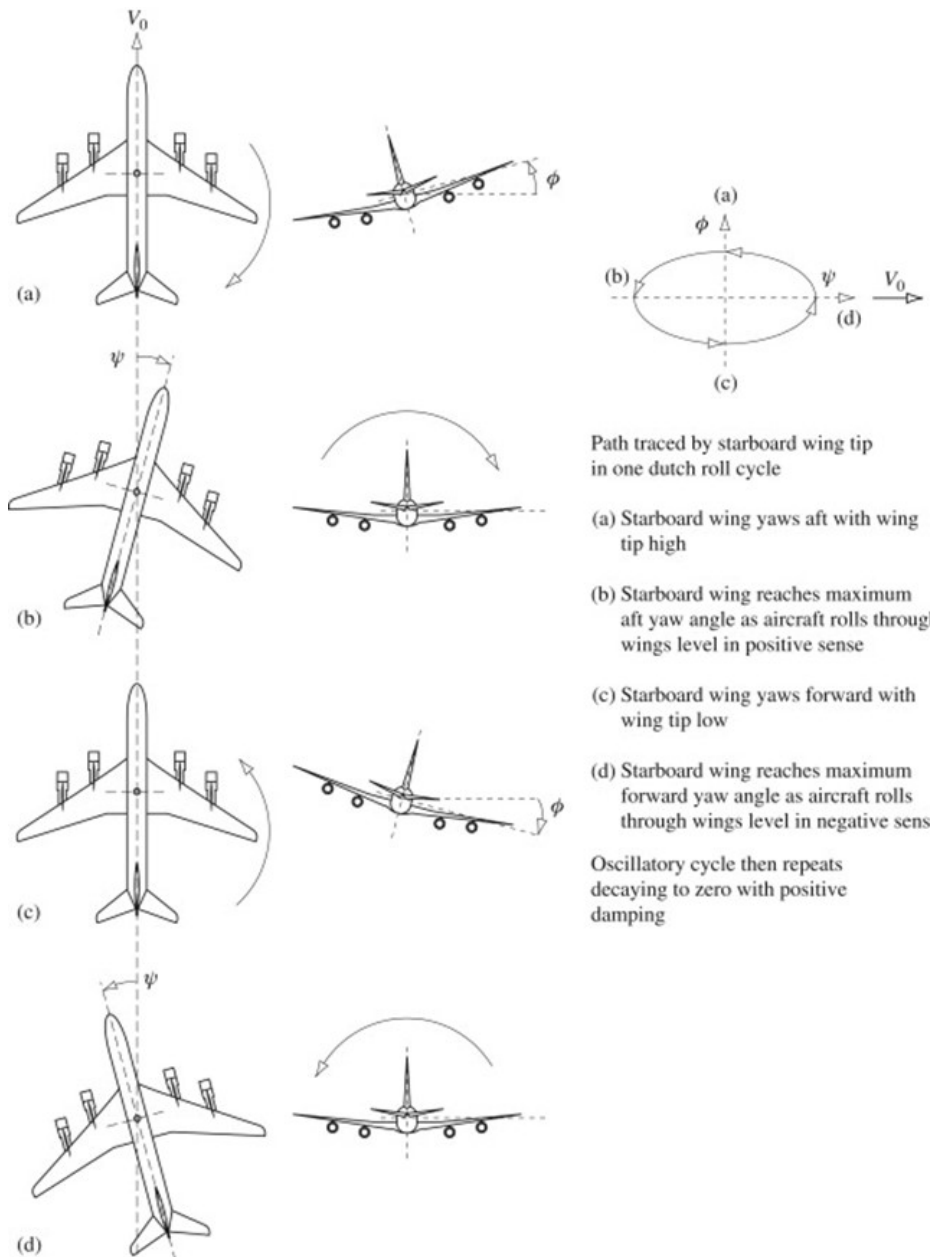


Figure E.2: Dutch Roll Schematic [7]

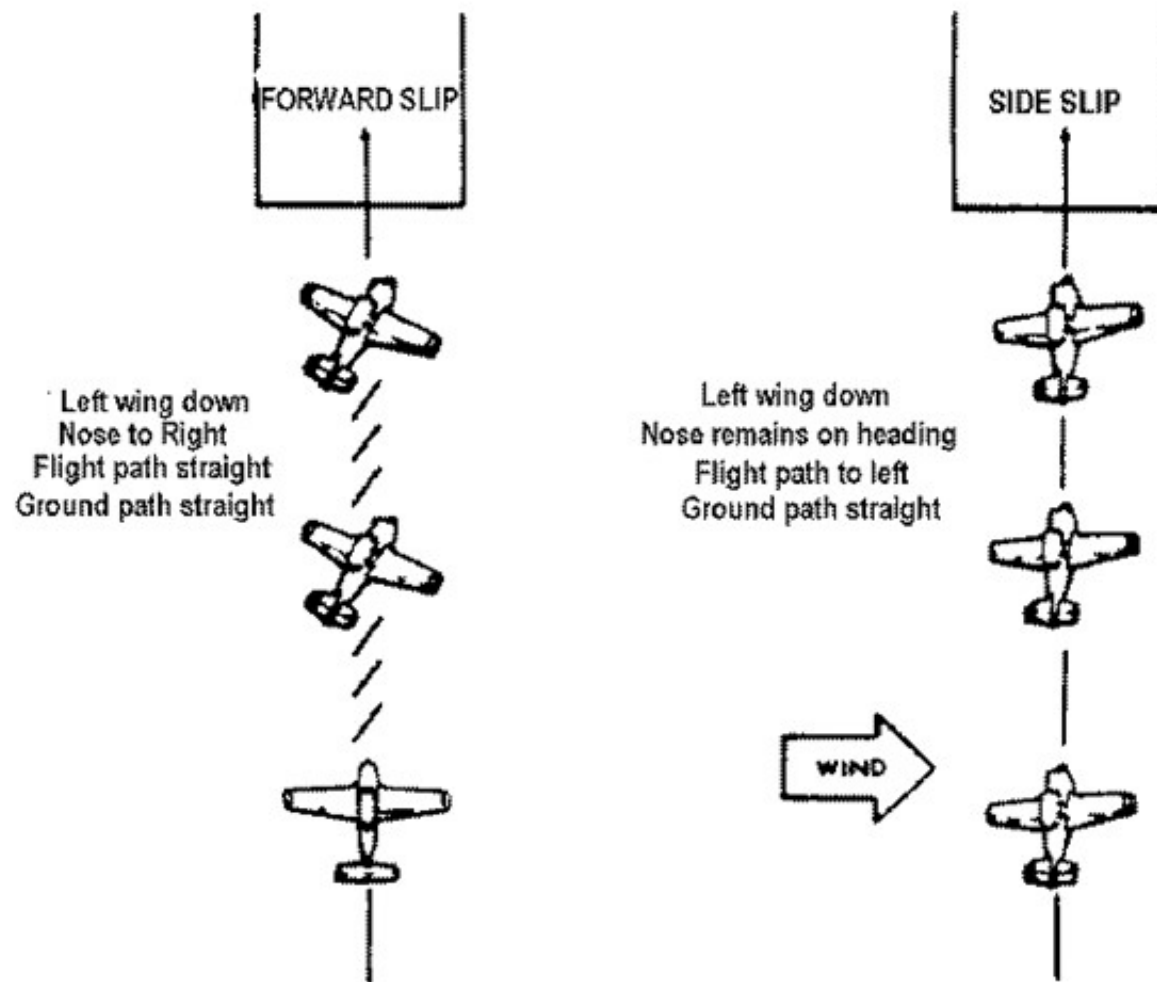
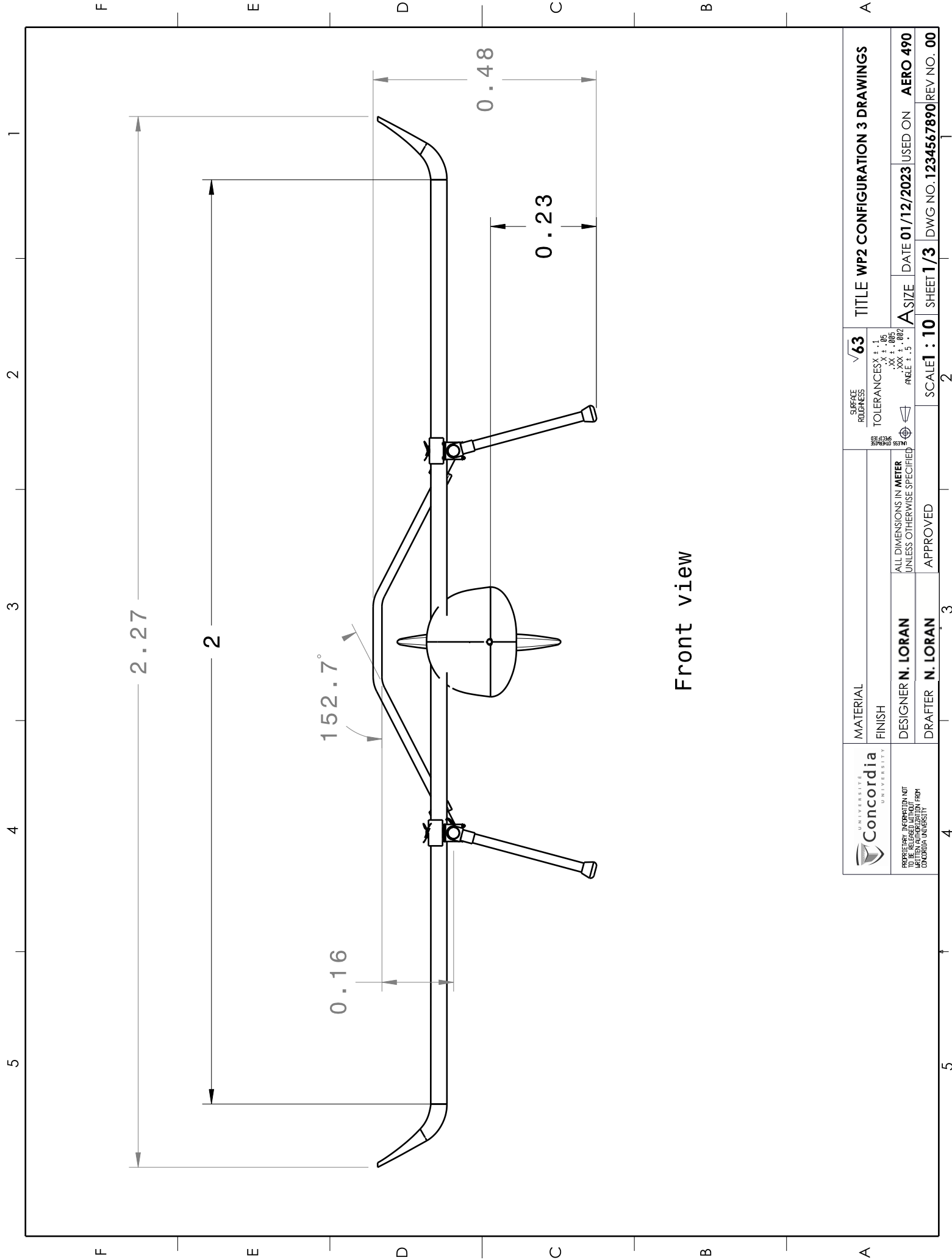


Figure 9-9 Forward Slip and Side Slip

Figure E.3: Sideslip schematic[5]

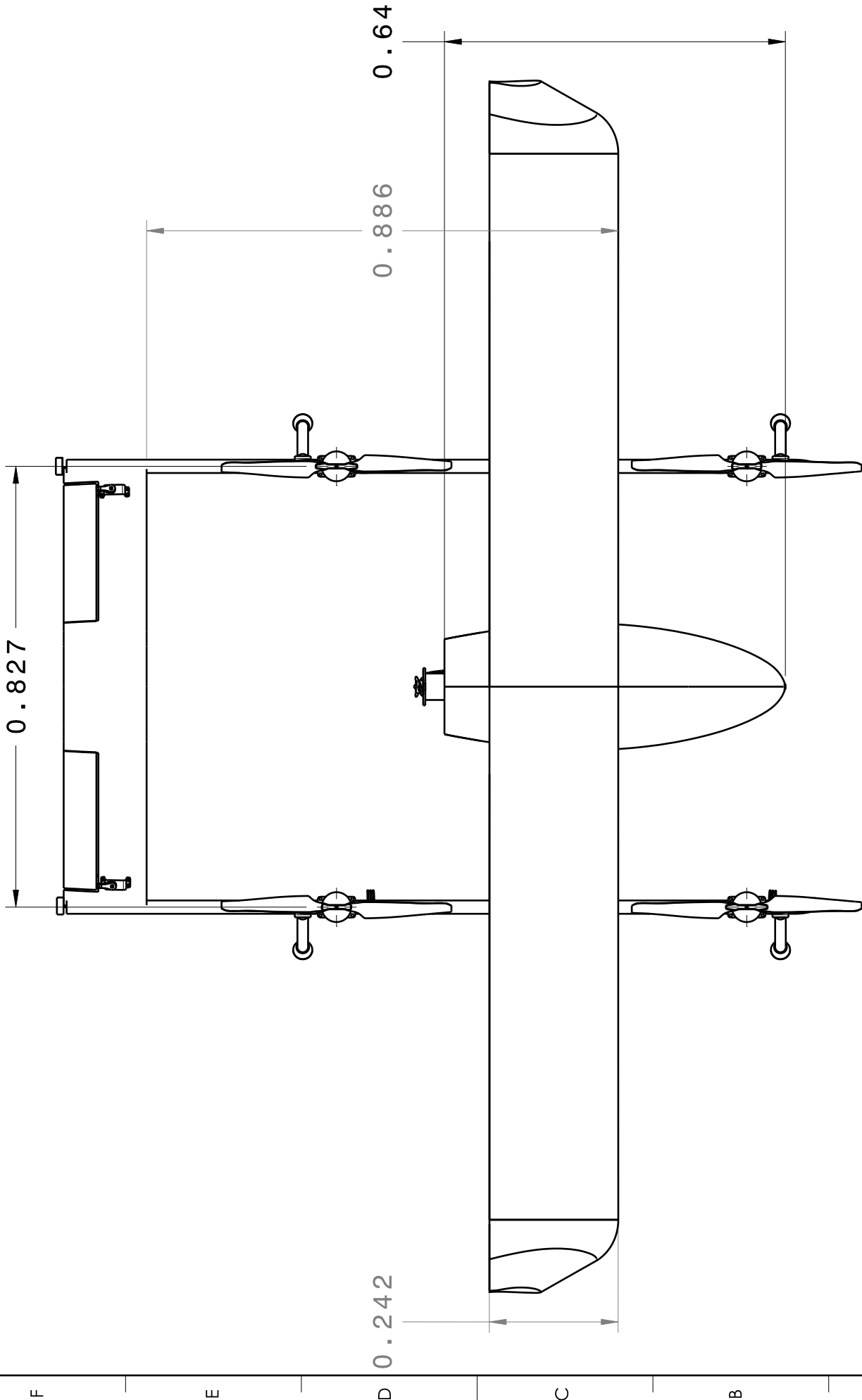
F Aircraft Drawings

Page left blank on purpose.



UNIVERSITÉ Concordia UNIVERSITY	MATERIAL FINISH	SURFACE ROUGHNESS $\sqrt{63}$	TITLE WP2 CONFIGURATION 3 DRAWINGS		
PROPRIETARY INFORMATION NOT TO BE RELEASED WITHOUT WRITTEN AUTHORIZATION FROM CONCORDIA UNIVERSITY	TOLERANCES X ± .15 YXX ± .005 ZXXX ± .002	ALL DIMENSIONS IN METER UNLESS OTHERWISE SPECIFIED	DATE 01/12/2023 USED ON AERO 490		
DESIGNER N. LORAN	ANGLE ± .5°	ASIZE	SCALE 1 : 10 SHEET 2/3	2	3
DRAFTER N. LORAN	APPROVED	4	DWG NO. 1234567890 REV NO. 00		

Top View



A

B

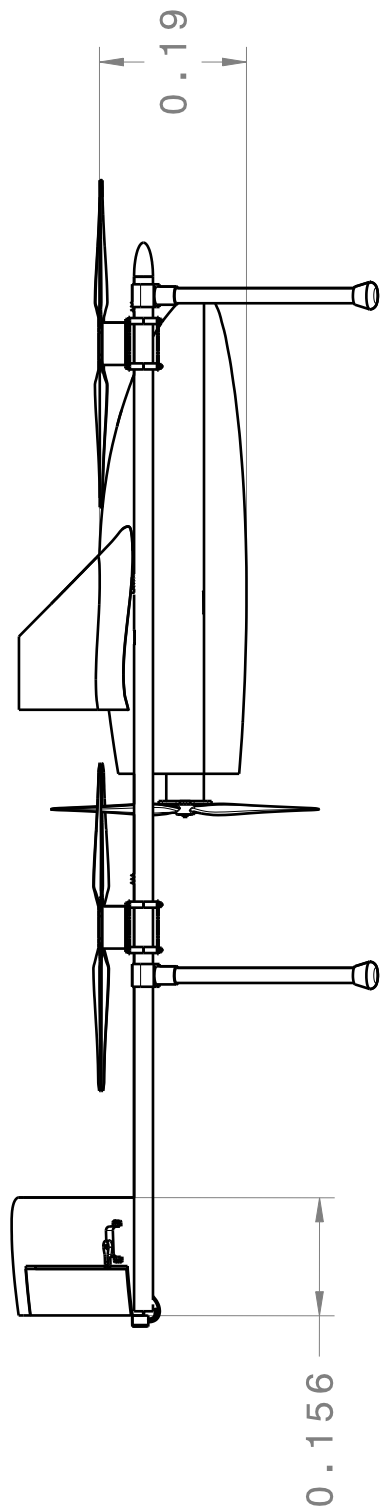
C

D

E

F

Right View



CONCORDIA UNIVERSITY		TITLE WP2 CONFIGURATION 3 DRAWINGS	
Concordia	MATERIAL	SURFACE ROUGHNESS $\sqrt{63}$	TOLERANCES IN METER
UNIVERSITY	FINISH	$X \pm .15$ $XX \pm .005$ $XXX \pm .002$	$A \pm .15$ ANGLE $\pm .5^\circ$
PROPRIETARY INFORMATION NOT TO BE RELEASED WITHOUT WRITTEN AUTHORIZATION FROM CONCORDIA UNIVERSITY	DESIGNER N. LORAN	ALL DIMENSIONS IN METER UNLESS OTHERWISE SPECIFIED	DATE 01/12/2023 USED ON AERO 490
	DRAFTER N. LORAN	APPROVED	SCALE 1 : 10 SHEET 3 / 3 DWG NO. 1234567890 REV NO. 00